Received: 10 July 2020 | Accepted: 29 August 2020

DOI: 10.1111/gcb.15339

PRIMARY RESEARCH ARTICLE

Global Change Biology WILEY

Current and future impacts of drought and ozone stress on Northern Hemisphere forests

Frederick Otu-Larbi[1] | Adriano Conte[2] | Silvano Fares[3] | Oliver Wild[1] | Kirsti Ashworth[1]

[1]Lancaster Environment Centre, Lancaster University, Lancaster, UK

[2]Council for Agricultural Research and Economics (CREA) – Research Centre for Forestry and Wood, Rome, Italy

[3]National Research Council (CNR) – Institute of BioEconomy (IBE), Rome, Italy

Correspondence
Frederick Otu-Larbi and Kirsti Ashworth, Lancaster Environment Centre, Lancaster University, Lancaster LA1 4YQ, UK.
Email: f.otu-larbi@lancaster.ac.uk (F. O.-L.); k.s.ashworth1@lancaster.ac.uk (K. A.)

Funding information
Lancaster University; Royal Society of London, Grant/Award Number: DH150070

Abstract

Rising ozone (O_3) concentrations, coupled with an increase in drought frequency due to climate change, pose a threat to plant growth and productivity which could negatively affect carbon sequestration capacity of Northern Hemisphere (NH) forests. Using long-term observations of O_3 mixing ratios and soil water content (SWC), we implemented empirical drought and O_3 stress parameterizations in a coupled stomatal conductance–photosynthesis model to assess their impacts on plant gas exchange at three FLUXNET sites: Castelporziano, Blodgett and Hyytiälä. Model performance was evaluated by comparing model estimates of gross primary productivity (GPP) and latent heat fluxes (LE) against present-day observations. CMIP5 GCM model output data were then used to investigate the potential impact of the two stressors on forests by the middle (2041–2050) and end (2091–2100) of the 21st century. We found drought stress was the more significant as it reduced model overestimation of GPP and LE by ~11%–25% compared to 1%–11% from O_3 stress. However, the best model fit to observations at all the study sites was obtained with O_3 and drought stress combined, such that the two stressors counteract the impact of each other. With the inclusion of drought and O_3 stress, GPP at CPZ, BLO and HYY is projected to increase by 7%, 5% and 8%, respectively, by mid-century and by 14%, 11% and 14% by 2091–2100 as atmospheric CO_2 increases. Estimates were up to 21% and 4% higher when drought and O_3 stress were neglected respectively. Drought stress will have a substantial impact on plant gas exchange and productivity, off-setting and possibly negating CO_2 fertilization gains in future, suggesting projected increases in the frequency and severity of droughts in the NH will play a significant role in forest productivity and carbon budgets in future.

KEYWORDS

Boreal forests, drought stress, forest productivity, future climate impacts, Mediterranean forests, ozone stress

1 | INTRODUCTION

Tropospheric ozone (O_3) concentrations have doubled in the Northern Hemisphere (NH) since the pre-industrial period (Yeung et al., 2019) and are currently increasing at a rate of 0.5%–2% per year due to changes in the release of precursor compounds from industrial activities (Gaudel et al., 2018; Hartmann et al., 2013). By the end of this century, NH tropospheric O_3 could increase by as much as 18% (Young et al., 2013) and drought frequency by 50%–200% (Zhao & Dai, 2017). Surface O_3 is a powerful phytotoxin (Ainsworth, Yendrek, Sitch, Collins, & Emberson, 2012; Ashmore, 2005). It enters leaves through the stomata and damages cell membranes, proteins and DNA through oxidation reactions (Leisner & Ainsworth, 2012; Omasa & Takayama, 2002). O_3 damages the photosynthetic apparatus affecting leaf gas exchange, leading to reductions in plant productivity, growth and biomass accumulation (Ainsworth et al., 2012; Paoletti, 2009).

Plants can respond to O_3-induced oxidative stress by closing stomata (an avoidance strategy), thus limiting water loss and stomatal O_3 flux, and by synthetizing antioxidants (a tolerance strategy) to regulate reactive oxygen species levels (Andersen, 2003; Pellegrini et al., 2019). Both tolerance and avoidance can be parameterized in vegetation models. The former assumes that plants can detoxify limited doses of O_3, thus reducing the oxidative stress. Such a pathway has been extensively described by several authors in the phytotoxic O_3 dose POD_y metric (De Marco et al., 2016; Emberson, Büker, & Ashmore, 2007; Mills, Hayes, et al., 2011; Mills, Pleijel, et al., 2011). In broad terms, the POD_y represents the cumulative quota of O_3 that a plant is not able to detoxify, and that is consequently harmful to the plant's ecophysiological processes. This approach has been shown to perform well across a variety of ecosystems in modelling studies (Clark et al., 2011; Sitch, Cox, Collins, & Huntingford, 2007). The latter strategy assumes that plants regulate stomata by directly reducing the exposure of internal plant tissues to O_3. It has been observed in many experiments that plants fumigated to high concentration of O_3 exhibit a general decrease in stomatal conductance (Wittig, Ainsworth, & Long, 2007). Hoshika, Watanabe, Inada, and Koike (2013) recently hypothesized that plants can optimize their stomatal behaviour to minimize O_3 influx and transpiration while maximizing carbon assimilation, and they reparameterized the optimal stomatal behaviour model developed by Medlyn et al. (2011). This optimal stomatal behaviour theory has also been shown to improve model estimates of photosynthesis and stomatal conductance on different seedling species in field experiments (Hoshika, Watanabe, et al., 2013) but has not been widely applied.

Although light and temperature are the main controls on instantaneous photosynthesis rates, drought stress is the limiting environmental factor for global plant photosynthesis and productivity (Nemani et al., 2003) and mortality, diminished growth and reduced productivity have all been observed in plants exposed to drought stress (Basu, Ramegowda, Kumar, & Pereira, 2016; Farooq, Wahid, Kobayashi, Fujita, & Basra, 2009). In response to drought stress, plants avoid oxidative and dehydrative damage to their cells by reducing their stomatal conductance to conserve water (Wilkinson & Davies, 2010), at the cost of reduced photosynthesis (Bréda, Cochard, Dreyer, & Granier, 1993; Clenciala, Kucera, Ryan, & Lindroth, 1998; Granier et al., 2007).

Both O_3 (Ainsworth et al., 2012; Leisner & Ainsworth, 2012) and drought stress (Nemani et al., 2003; Osakabe, Osakabe, Shinozaki, & Tran, 2014) reduce plant growth and productivity thereby reducing the carbon uptake of NH forests. While many studies have focused on the effects of either drought (Egea, Verhoef, & Vidale, 2011; Keenan et al., 2010) or O_3 (Ashmore, 2005; Büker et al., 2015; Emberson, Ashmore, Cambridge, Simpson, & Tuovinen, 2000) stress on forest productivity and gas exchange, few have looked at how these two stressors interact (e.g. Grüters, Fangmeier, & Jäger, 1995; Hoshika, Omasa, & Paoletti, 2013). As drought induces stomatal closure, it is generally thought to minimize O_3 damage since reduced stomatal conductance would reduce stomatal O_3 deposition and uptake (Panek & Goldstein, 2001). However, the interaction between drought stress and O_3 exposure is complex and while some studies show no significant interaction between the two stressors (Wittig, Ainsworth, Naidu, Karnosky, & Long, 2009), others have shown additive effects with O_3-induced loss of stomatal regulation increasing drought stress impact (Paoletti & Grulke, 2010).

The complexity of modelling O_3 and drought stress impacts on vegetation is compounded by the differing levels of sensitivity of different ecosystems. Mediterranean climates are characterized by high temperature, strong insolation and prolonged drought during the summer, conditions which promote photochemical tropospheric O_3 formation (Millán et al., 2000; Paoletti, 2006). These conditions are expected to increase in frequency and intensity in future (IPCC, 2013). Vegetation in this region has developed adaptations to such stresses, for example, leaf morphology, water conservation by reduced transpiration and the synthesis and emission of biogenic volatile organic compounds including powerful antioxidants and compatible solutes (Calfapietra, Fares, & Loreto, 2009; Nali et al., 2004; Paoletti, 2006), and may therefore be better able to tolerate such stressors. By contrast, Boreal climates have mild wet summers and cold winters, leading to generally low O_3 concentrations and infrequent droughts. Hence, Boreal forests have not developed strategies to avoid or tolerate either stress and may be more vulnerable to damage than Mediterranean forest ecosystems. These contrasting characteristics make Mediterranean and Boreal ecosystems ideal for testing the effect of droughts and O_3 on NH forests. As they also make up 9.4% (M'Hirit, 1999) and 17% (Kasischke, 2000) of the Earth's land surface area, respectively, changes in their productivity could have major implications for the global carbon cycle.

Vegetation models play an important role in predicting likely impacts of climate change on forest productivity, but confidence in future projections is dependent on their performance when evaluated against present-day observations. We test the skill of a one-dimensional canopy-exchange model (FORest Canopy-Atmosphere Transfer [FORCAsT]; Ashworth et al., 2015) to reproduce observed

carbon assimilation via gross primary productivity (GPP) and water loss via latent heat fluxes (LE) at sites in two Mediterranean and one Boreal evergreen forests.

Here, we investigate the implications of increasing O_3 and drought events for carbon sequestration by the middle (2041–2050) and end (2091–2100) of the 21st century under Representative Concentration Pathway RCP8.5. Our objectives are to determine: (a) defensive strategies used against O_3 stress in Mediterranean and Boreal forests under present-day conditions, (b) the relative contributions and possible interactions of drought and O_3 stress to changes in plant gas exchange, and (c) the potential impacts of future changes in SWC and O_3 concentrations on gas exchange and hence productivity.

2 | METHODS

2.1 | FORCAsT model

FORCAsT is a 1D model of biosphere–atmosphere chemical exchange which has previously been used to study canopy structure and mixing (Bryan et al., 2012, 2015), stomatal regulation and atmospheric chemistry within and above forest canopies (Ashworth et al., 2015, 2016) and the impact of drought stress on biogenic volatile organic compound emissions and forest gas exchange (Otu-Larbi, Bolas, et al., 2020). A full description of the FORCAsT model can be found in Ashworth et al. (2015). Three different coupled photosynthesis-stomatal conductance (A–g_s) models have since been incorporated into FORCAsT giving users the flexibility to select the most appropriate for the ecosystem of interest and the meteorological and physiological observations available (see Otu-Larbi, Conte, et al., 2020 [in preparation] for full details).

Here, we describe the parameterizations of drought and O_3 stress used in this study. We apply the Medlyn et al. (2011) optimal stomatal behaviour modification of the Farquhar, Von Caemmerer, and Berry (1980) photosynthesis model in which photosynthesis rate (A; μmol m^{-2} s^{-1}) is the minimum of two limiting factors: electron transport and carboxylation rate. Stomatal conductance (g_s) is modelled assuming that stomatal aperture is regulated to maximize carbon gain while simultaneously minimizing water loss (Medlyn et al., 2011):

$$g_s \approx g_o + \left(1 + \frac{g_1}{\sqrt{D}}\right)\frac{A}{C_s}, \quad (1)$$

where g_o (mol m^{-2} s^{-1}) is the residual stomatal conductance when A approaches zero and g_1 is a fitted parameter representing the sensitivity of g_s to A. The values of g_o and g_1 are determined at the species- or plant functional type (PFT)-specific level from experimental data. Here, we use values obtained from Lin et al. (2015) and De-Kauwe et al. (2015), respectively, as indicated in Table S1. D (kPa) is the vapour pressure deficit calculated by FORCAsT and C_s (μmol/mol) is the CO_2 concentration at the leaf surface.

LE (W/m^2) is estimated following Lhomme, Elguero, Chehbouni, and Boulet (1998) as:

$$\left(\frac{\rho C_p}{\gamma}\right) ge_v \left(e_s - e_a\right), \quad (2)$$

where ρ (kg/m^3) is the air density, C_p (J kg^{-1} K^{-1}) is the specific heat capacity of air at constant pressure, γ (kPa/K) is the psychrometric constant (the ratio of C_p to latent heat of vaporization of water), e_s and e_a (kPa) are the saturated vapour pressure at leaf temperature and the air water vapour pressure, respectively, and ge_v (m/s) is an equivalent conductance for horizontal vapour transfer estimated as:

$$ge_v = 2LAI_i\left(\frac{g_{bw}g_{sw}}{g_{bw}+g_{sw}}\right), \quad (3)$$

where LAI_i (m^2/m^2) is the leaf area index at model layer i, g_{bw} (mol m^{-2} s^{-1}) and g_{sw} (mol m^{-2} s^{-1}) are the leaf boundary layer and stomatal conductance to water respectively.

2.2 | Soil moisture stress

Accounting for drought stress impacts on plants in vegetation models is challenging. The response depends on soil characteristics, climatic conditions and PFT. Metrics based on SWC, soil water potential and predawn leaf water potential have all been developed to assess plant water status (e.g. see Keenan et al., 2010; Zhou et al., 2014). Predawn leaf water potential provides the best measure of plant water status, but the lack of long-term observations makes these metrics difficult to apply in modelling studies. In contrast, SWC, while not as robust, is measured at most forest sites and can also be derived from satellite data making it easier to use in model parameterizations and simulations.

In this study, the effect drought stress on A and g_s is assumed to be the result of biochemical and stomatal limitations as demonstrated in previous studies (e.g. see Egea et al., 2011). A soil moisture stress function was incorporated into the photosynthesis module in FORCAsT as described by Otu-Larbi, Conte, et al. (2020). The stress function, β, ranges between 1 (in the absence of drought stress) and 0 (at wilting point) and is calculated from:

$$\beta = \begin{cases} 1 & \text{for} \quad \theta \geq \theta_c \\ \left[\dfrac{(\theta-\theta_w)}{(\theta_c-\theta_w)}\right]^q & \text{for } \theta_w < \theta < \theta_c \\ 0 & \text{for} \quad \theta < \theta_w \end{cases}, \quad (4)$$

where θ (m^3/m^3) is the volumetric soil moisture, θ_w is the wilting point (m^3/m^3) and θ_c is a critical soil moisture content above which drought stress is found not to affect plant–atmosphere gas exchange (Egea et al., 2011; Keenan et al., 2010). q is a site-specific empirical factor

describing the non-linearity of the effects of soil drought stress on tree physiological processes. θ_c, θ_w and q were calculated from soil texture data (i.e. sand, clay and silt fractions) or calibrated using long-term soil moisture observations at each site as detailed in Otu-Larbi, Conte, et al., 2020 and provided in Table S1.

The water-stressed values of carboxylation (V_{cmax*}) and electron transport (J_{max*}) rate are then calculated from the maximum rates (V_{cmax} and J_{max}) as:

$$V_{cmax^*} = V_{cmax} \times \beta, \tag{5a}$$

$$J_{max^*} = J_{max} \times \beta, \tag{5b}$$

and these values are applied to calculate the impact of soil moisture deficit on photosynthesis. The stomatal conductance then becomes:

$$g_s \approx g_o + \left(1 + \frac{g_{1\beta}}{\sqrt{D}}\right)\frac{A}{C_s}. \tag{6}$$

2.3 | Incorporating O_3 damage

The reduction in photosynthesis and plant productivity due to O_3 cellular damage is incorporated into FORCAsT following two assumed strategies.

2.3.1 | O_3 avoidance (AVD)

O_3 avoidance (stomatal closure) follows Hoshika, Watanabe, et al. (2013). The details of the mathematical formulation are provided in Medlyn et al. (2011) and Hoshika, Watanabe, et al. (2013) and only a short summary is given here. The O_3 flux through the stomata (F_{st}: mol m^{-2} s^{-1}) is given by:

$$F_{st} = \frac{g_s}{1.6}\left([O_3]_{air} - [O_3]_{leaf}\right), \tag{7}$$

where $[O_3]_{air}$ is the ambient O_3 concentration (ppbv) and $[O_3]_{leaf}$ is the O_3 concentration inside the leaf, usually assumed negligible (e.g. Laisk et al., 1989). 1.6 is the ratio of the diffusion coefficients of water vapour and O_3.

In the optimal stomatal behaviour theory, the control of leaf gas exchange may be considered optimal when it maximizes carbon gain while simultaneously minimizing water loss. Assuming stomata act to minimize O_3 damage in a similar manner, then the optimal stomatal conductance can be found from a modification of Equation (6):

$$g_s \approx g_o + \left(1 + \frac{g_1 \beta}{\sqrt{D + (k/1.6)[O_3]_{air}}}\right)\frac{A}{C_a}, \tag{8}$$

where k (mol H_2O/mol O_3) is the ratio of the marginal water cost of plant carbon gain to the marginal O_3 damage of plant carbon gain and is calculated as:

$$0.1\frac{1.6D}{[O_3]_{air}} < k < \frac{1.6D}{[O_3]_{air}}, \tag{9}$$

where D and $[O_3]_{air}$ are the long-term mean VPD (kPa) and $[O_3]_{air}$ respectively. The value of k for each site is provided in Table S1.

2.3.2 | O_3 tolerance (TLR)

Plants' strategy to tolerate O_3 consists of enzymatic processes and chemical reactions to detoxify photooxidants. O_3-tolerant trees (e.g. *Pinus strobus*) have been shown to have higher glutathione reductase and ascorbate peroxidase than O_3-sensitive species (Chevone, 1991). This prevents oxidative damage to the photosystem, enabling plants to maintain photosynthesis at higher doses of O_3. Here, we assume that the instantaneous uptake of O_3 by plants only leads to an immediate suppression of leaf photosynthesis above a critical stomatal O_3 flux threshold. The decrease in leaf photosynthesis from its potential maximum is therefore proportional to the flux above that critical flux. The reduction factor, F, is calculated following Pleijel et al. (2004) as:

$$F = 1 - \alpha.\max\left[F_{O_3} - Y, 0\right], \tag{10}$$

where F_{O_3} (nmol m^{-2} s^{-1}) is the instantaneous flux of O_3 into the leaf, α (mmol^{-1} m^{-2}) is a PFT-specific parameter indicating the fractional reduction of photosynthesis with O_3 uptake by leaves and Y is the PFT-specific O_3 flux threshold above which O_3 damage occurs. In this study, we use α values of 0.04 and 0.02 for broadleaf and needleleaf trees respectively (Clark et al., 2011) and a threshold of 1 nmol m^{-2} s^{-1} for forest trees as recommended by Mills, Hayes, et al. (2011) and Mills, Pleijel, et al. (2011). F_{O_3} is calculated as:

$$F_{O_3} = \frac{[O_3]\ air}{r_a + kO_3/g_s}, \tag{11}$$

where $[O_3]_{air}$ is the ambient O_3 concentration (ppbv), r_a (s/m) is the combined aerodynamic and boundary layer resistance of the leaf surface, kO_3 (1.67) is the ratio of the leaf resistance for O_3 to water vapour (Sitch et al., 2007) and g_s (m/s) is the leaf conductance for H_2O.

The O_3-affected values of photosynthesis rate (A^*) and stomatal conductance (g_s^*) are estimated as:

$$A^* = A \times F, \tag{12a}$$

$$g_s^* = g_s \times F, \tag{12b}$$

where A and g_s are the (potential) photosynthesis rate and stomatal conductance in the absence of O_3.

2.4 | Scaling up to the canopy

GPP is estimated as:

$$GPP = A_n + R_d, \quad (13)$$

where A_n (μmol m^{-2} s^{-1}) is the net photosynthesis (including the effects of drought and O_3 stress) and R_d (μmol m^{-2} s^{-1}) is the canopy dark respiration which is estimated by the model. Leaf-level A_n, GPP and LE in each layer of the canopy (i) were scaled by LAI at each model level (LAI_i) and summed over all model layers (n) to obtain canopy-scale (c) estimates of A, GPP and LE.

$$A_c = \sum_{i=1}^{n} A_i \times LAI_i, \quad (14a)$$

$$GPP_c = \sum_{i=1}^{n} GPP_i \times LAI_i, \quad (14b)$$

$$LE_c = \sum_{i=1}^{n} LE_i \times LAI_i. \quad (14c)$$

2.5 | Study sites and data

Three evergreen NH forest sites with long-term continuous measurements of meteorology, O_3 concentrations, GPP and LE fluxes were used in this study: a Holm oak forest at Castelporziano (CPZ; Fares, Alivernini, Conte, & Maggi, 2019), a Boreal pine forest at Hyytiälä (HYY; Hari et al., 2013) and a Ponderosa pine forest at Blodgett (BLO; Sorooshian, Li, Hsu, & Gao, 2012). These sites are part of the FLUXNET network (Pastorello et al., 2017). Full details of the sites, and the data and model parameters used are provided in Table S1.

Observations of photosynthetically active radiation (PAR; μmol m^{-2} s^{-1}), air temperature (K), CO_2 concentration (ppm), volumetric SWC (m^3/m^3), wind speed (m/s) and direction (degrees clockwise from North), relative humidity (RH; %) and atmospheric pressure (Pa) were obtained for each site from the FLUXNET-2015 data set at a temporal resolution of 30 min. O_3 data were obtained directly from site lead investigators. The number of years for which data are available at each site is given in Table S1.

The Castelporziano Estate (41°42′N, 12°21′E) is located 25 km SW of Rome, Italy, and 1.5 km from the Mediterranean coast. The forest is dominated by evergreen Holm oak (*Quercus ilex*), and the average LAI and mean tree height are 3.69 m^2/m^2 and 16 m respectively (Fares et al., 2019). The climate at CPZ is classified as Csa (Mediterranean: mild with dry, hot summer) according to the Koppen climate classification (Köppen, 1923). Precipitation mainly occurs in autumn and winter with little or none in the summer, resulting in annual droughts. Average soil moisture (Figure 1) drops from 0.20 m^3/m^3 in the winter and spring to ~0.10 m^3/m^3 during

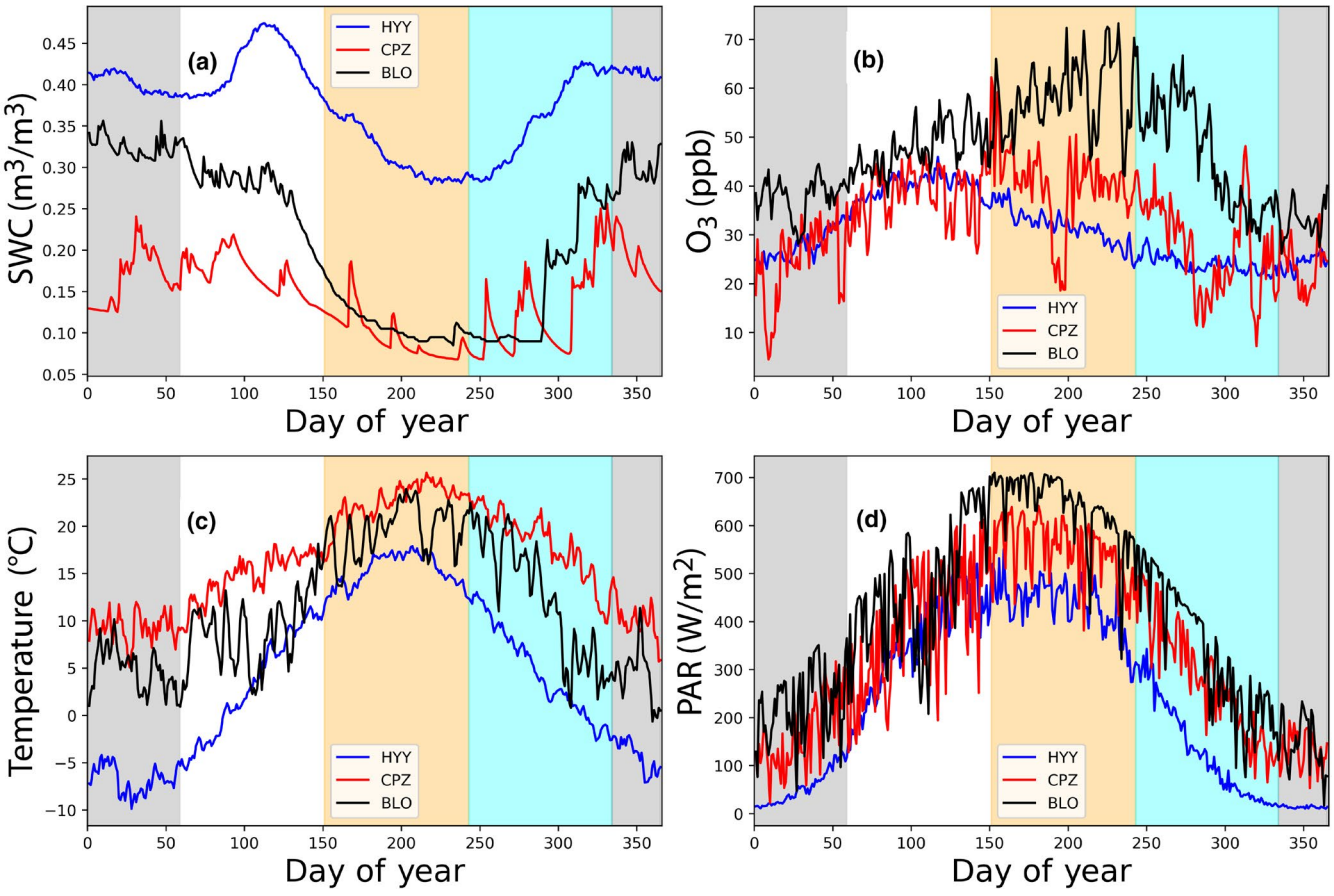

FIGURE 1 Average annual profiles of observed (a) volumetric soil water content (SWC), (b) O_3 mixing ratios, (c) air temperature and (d) photosynthetically active radiation at: Castelporziano (CPZ; red lines), Hyytiälä (HYT; blue lines) and Blodgett (BLO; black lines). The coloured backgrounds denote meteorological seasons: winter (grey), spring (white), summer (orange) and autumn (cyan)

the summer. The long-term (1997–2009) annual average precipitation is 780 mm and the mean temperature is 15.6°C. As shown in Figure 1, O_3 mixing ratios in this ecosystem exhibit strong seasonality with higher concentrations observed during the warm, dry summer months (up to 50 ppb) than the winter (as low as 20 ppb). Similarly, PAR has higher values in the summer (~600 W/m^2) than winter (~100 W/m^2).

BLO Forest (38°53′N 120°37′W) is located at 1,315 m a.s.l. in the Sierra Nevada Mountains of California, United States. Ponderosa pine (*Pinus ponderosa* L.) dominates with average LAI and tree height of 3.20 m^2/m^2 and 6 m (Law & Gower, 2001) respectively. This site also has a Koppen climate classification of Csa; the summers are dry with rainfall only occurring in the winter and spring (except during 2003 and 2004 when 38 and 22 mm of summer rain fell respectively). Data from 1997 to 2007 show an annual mean precipitation and temperature of 1,230 mm and 11.1°C respectively. Summer drought is a yearly occurrence. Figure 1 shows that soil moisture content follows the precipitation pattern with a peak of ~0.30 m^3/m^3 in the winter–spring and a summer low of ~0.10 m^3/m^3. The seasonal pattern of PAR, temperature and O_3 concentrations is similar with highest values in the summer and lowest in winter.

The Station to Measure Ecosystem–Atmosphere Relations (SMEAR II) located in HYY, Finland (61°51′N, 24°17′E; 181 m a.s.l.; Hari & Kulmala, 2005), is a Boreal coniferous forest with a Koppen climate classification of Dfc (Continental subarctic climate). Seventy-five percent of this forest constitutes Scots pine (*Pinus sylvestris*) with Norway Spruce (*Picea abies*) and deciduous trees making up the remainder (Zhou et al., 2017). Average LAI is ~2.7 m^2/m^2 and the canopy height is ~23 m. Average annual mean air temperature and precipitation are 3.8°C and 709 mm, respectively, for the period 1996–2014. Droughts are infrequent but occurred here during 2003 (Ciais et al., 2005) and 2006 (Gao et al., 2016). Temperature and PAR peak in the summer. O_3 mixing ratios are lowest in the winter (25 ppb) and reach a peak of 40 ppb during spring. Soil moisture is highest in spring (~0.45 m^3/m^3) and lowest in summer (~0.30 m^3/m^3). Further details of the canopy and site characteristics can be found in Hari and Kulmala (2005) and Hari et al. (2013).

2.6 | Impact of future changes in SWC and O_3 concentrations

We investigate the potential impacts of climate change on GPP and LE fluxes in the middle (2041–2050) and end (2091–2100) of the 21st century. Monthly mean data for surface O_3 mixing ratios, SWC, solar radiation, RH, wind speed, Pa, temperature and carbon dioxide (CO_2) were obtained from general circulation models (GCMs) participating in the 5th Phase of the Coupled Model Intercomparison Project (CMIP5; Taylor, Stouffer, & Meehl, 2012) and Atmospheric Chemistry and Climate Model Intercomparison Project. Output from different participating models differs in space and time (Taylor et al., 2012; see https://portal.enes.org/data/enes-model-data/cmip5/resolution for a list of models and their characteristics). Only the seven models (from five modelling centres) that provide both O_3 mixing ratios and SWC were selected. Details of these are provided in Table S2.

Variables were obtained from historical GCM simulations for 1850–2005 and GCM future simulations for 2006–2100 following RCP8.5, a scenario in which emissions of CO_2 follow an exponential growth trajectory throughout the century (Riahi et al., 2011), with concentrations increasing to 936 ppm and nominal anthropogenic forcing to 8.5 W/m^2 by 2100 (IPCC, 2014).

Comparing historical model output and observations shows systematic (but differing) biases in all seven models (see Figure S1). We used historical data for 1996–2005 (corresponding to our observations) to bias-correct each model for 2006–2100, before applying it to drive FORCAsT simulations. We calculated monthly averages for each variable at each site from both observations and GCM data for the 1996–2005 period. Monthly relative bias correction factors were calculated for each variable and month as follows:

$$\mathrm{RBF}_i = \frac{\mathrm{OBS}_i}{\mathrm{HMOD}_i}, \tag{15}$$

where RBF_i, OBS_i and HMOD_i represent the relative bias factor, observed values and historical model output value of a variable for each month, *i*.

Future GCM model output for 2041–2050 and 2091–2100 was then bias corrected assuming that historical and future model biases are similar:

$$\mathrm{BC}_i = \mathrm{FMOD}_i \times \mathrm{RBF}_i, \tag{16}$$

where BC_i is the bias-corrected data, FMOD_i is the original GCM future projection and RBF_i is the relative bias correction factor for month of the year, *i*. The bias-corrected data for each site are shown in Figures S2–S4.

2.7 | Model configurations and experiments

We evaluate FORCAsT performance and determine the most suitable O_3-stress response strategy at each site from present-day simulations, driven with site observation data. FORCAsT simulations driven by future climate are used to investigate potential changes in forest productivity due to future changes in drought and O_3 stress. Six model simulations were performed for each site. An initial control (CTR) simulation was run without either O_3 or drought stress and modelled GPP and LE were compared against observations. We then tested the effect of drought stress only (CTR + Dr) and each of the O_3-stress responses (TLR and AVD), comparing the results of each simulation against CTR as well as observations. Finally, we tested the impact of combining O_3 and drought stress (AVD + Dr and TLR + Dr). Although observations at HYY span the period from 1997 to 2014, we use data for only 2 years for consistency with CPZ and BLO. We select 2005–2006

for the analysis because 2006 was a drought year (Gao et al., 2016) and therefore allows for assessment of drought impact. An evaluation of FORCAsT performance at HYY for the entire 1997–2014 period is shown in Figure S5.

Four simulations were conducted using bias-corrected future meteorological data from each GCM model at each site to test the impact of drought and O_3 on GPP and LE fluxes. These simulations tested the effects of (a) not accounting for either O_3 or drought stress in the model (FUT), (b) including only drought stress (FUT + Dr), (c) including only O_3 stress (FUT + O_3) and (d) including both (FUT + DrO_3). The O_3 impacts were modelled using the strategy that provided the best present-day model-observation fit.

3 | RESULTS

Droughts occur almost annually at BLO and CPZ but rarely at HYY, as shown in Figure 1. O_3 concentrations are also higher at the Mediterranean sites. We present the impacts of drought and O_3 stress on modelled GPP and LE under present-day conditions in Section 3.1. Model performance is evaluated against observed GPP and LE fluxes for the three sites from the FLUXNET-2015 data set. We determine the relative magnitude of the impacts of drought and O_3 on modelled GPP and LE and assess which defensive mechanism (tolerance [TLR] or avoidance [AVD]) is most appropriate for each ecosystem. Section 3.2 focuses on the potential impacts of drought and O_3 stress on future GPP and LE and the implications for future carbon sink.

3.1 | Current impacts of drought and O_3 on GPP and LE

Table 1 and Figure 2 show the annual average observed and simulated GPP and LE for each site calculated for each 2-year simulation period. Under present-day conditions, CPZ and BLO are more productive than HYY; observed GPP at HYY was about half of that observed at CPZ and ~70% of that at BLO. LE at BLO was approximately 35% and 60% higher than the observed values at CPZ and HYY respectively.

TABLE 1 Summary of observed and modelled annual cumulative gross primary productivity (GPP) and latent heat fluxes (LE) in present-day simulations. Observations (OBS) and best-fit model simulations are highlighted in bold

	Cumulative GPP (g C m^{-2} $year^{-1}$)			Cumulative LE (W m^{-2} $year^{-1}$)		
SITE	CPZ	BLO	HYY	CPZ	BLO	HYY
OBS	**2,120**	**1,629**	**1,084**	**305**	**465**	**196**
CTR	2,774	2,191	1,382	402	604	231
CTR + Dr	2,306	1,900	1,244	324	535	210
AVD	2,749	2,093	1,377	380	552	220
AVD + Dr	2,291	1,818	1,239	311	**495**	**201**
TLR	2,543	2,020	1,347	372	569	226
TLR + Dr	**2,171**	**1,772**	**1,217**	**308**	510	207

In general, FORCAsT overestimated GPP and LE across all three sites in CTR simulations when the effects of stress were excluded. Model overestimation was higher when drought stress was excluded (CTR) than O_3 stress irrespective of whether TLR or AVD was assumed. Drought stress has a greater impact on model estimates of GPP and LE at CPZ and BLO than at HYY due to the lower SWC and frequent drought at these sites. At CPZ and BLO, the inclusion of drought stress alone in FORCAsT (CTR + Dr) led to a 20% average reduction in model overestimation of GPP and LE but only a 10% reduction at HYY.

The impact of including O_3 stress differed between individual sites and the choice of O_3 stress parameterization adopted but generally improved the model fit to observations for both GPP and LE compared to CTR simulations. O_3 stress alone produced better agreement between modelled and observed GPP at all sites when tolerance rather than avoidance was assumed. For example, while TLR led to 11% reduction in model overestimation of GPP at CPZ, AVD only led to a 1% reduction. Like drought stress, O_3 stress alone has greater impacts on plant productivity at the Mediterranean forests than the Boreal forest.

Inclusion of drought and O_3 stress in the model (AVD + Dr and TLR + Dr) produced the lowest deviations and hence the best fit to observations at all study sites for both GPP and LE. For GPP, TLR + Dr simulations, shown in grey bars, fitted the observations better at all sites. LE estimates from AVD + Dr provided lower deviations from observations at BLO and HYY while TLR + Dr was the closest to observed values at CPZ. The combined effect of the two stresses was less than the sum of the individual stresses at all sites. For example, while CTR + Dr and TLR led to 22% and 11% reductions in GPP, respectively, their combined effect (TLR + Dr) was ~5% less (a 28% reduction). Similar results were obtained for all sites for both TLR and AVD parameterizations.

The Taylor diagrams (Taylor, 2001) presented in Figure 3 show three model performance statistics: correlation coefficient (*r*: blue lines), normalized standard deviation (*SD*: black dashed lines) and centred root-mean-square error (RMSE; orange dashed lines). A model simulation which exactly reproduces observations would lie on top of the observations (indicated by a purple dot on Figure 3). Therefore, the closer a model's performance statistics are to that of the observations on the Taylor diagram, the better its performance. Figure 3 shows high correlation coefficients for all model simulations for both GPP (0.85–0.98) and LE (0.88–0.95) indicating that FORCAsT reproduces the observed seasonal cycles for all sites. At CPZ, FORCAsT simulations showed better correlation with observations for LE than GPP (Figure 3a,d) whereas the reverse was true at both BLO and HYY. *SD* and RMSE were lower for both GPP and LE across all sites when drought stress was included (i.e. CTR + Dr, AVD + Dr and TLR + Dr), further confirming the results shown in Figure 2. As seen from Figures 2 and 3 and Table 1, TLR + Dr simulations had the lowest deviations between model and observations in addition to high correlation coefficients and lower RMSE suggesting

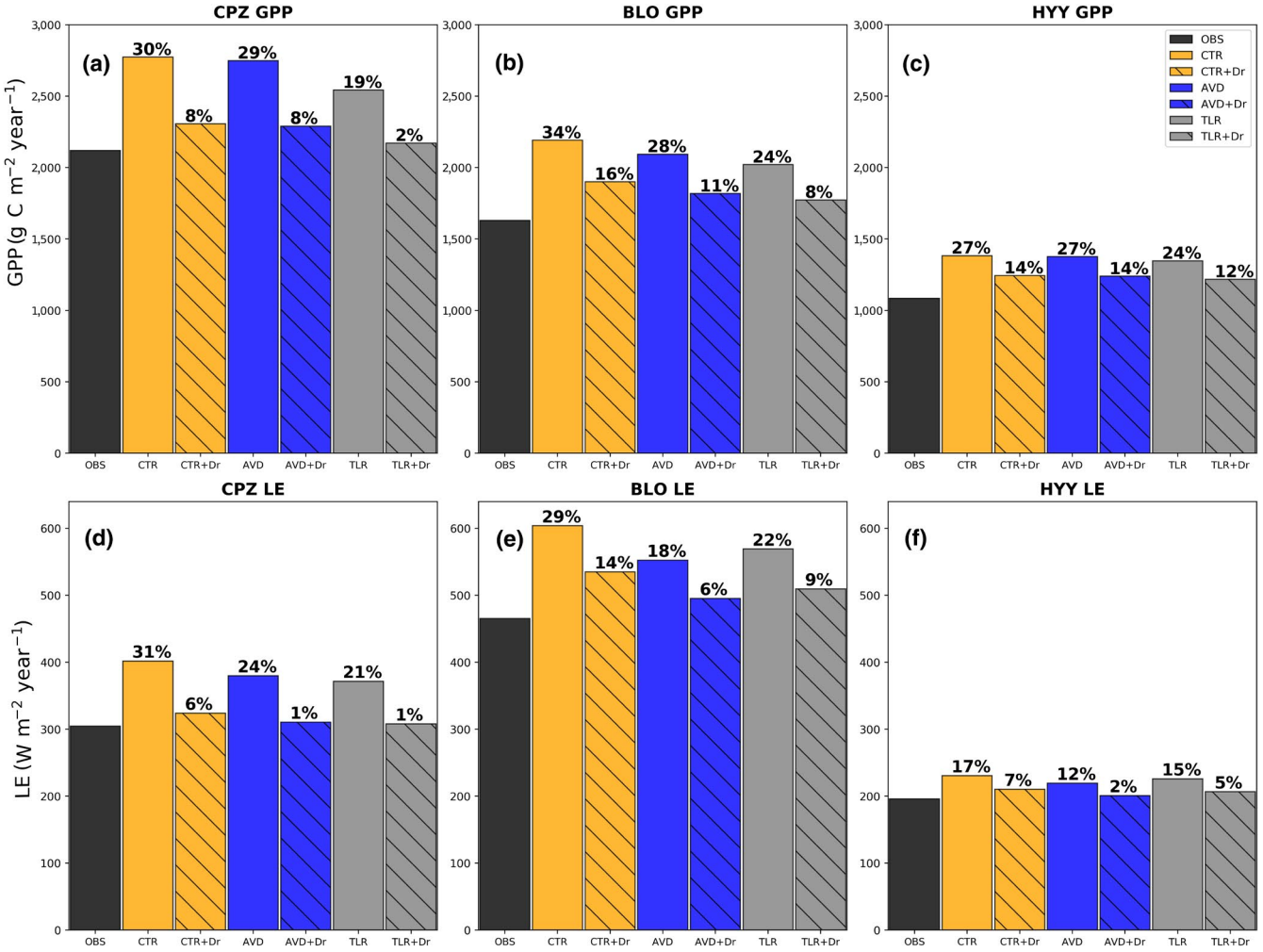

FIGURE 2 Annual mean gross primary productivity (GPP) (a–c) and latent heat flux (LE) (d–f) for Castelporziano (CPZ), Blodgett (BLO) and Hyytiälä (HYY). Observed (OBS) values are shown with black bars while model results are coloured as follows: orange (CTR and CTR + Dr), blue (AVD and AVD + Dr) and grey (TLR and TLR + Dr), with striped bars indicating drought stress. The percentage difference between modelled and observed values for each simulation is shown at the top of the bars. Positive values indicate model overestimation

that this is the best model parameterization for estimating GPP. For LE, TLR + Dr performed better at CPZ than any other model configuration while AVD + Dr provided the best model-observation fit at BLO and HYY. Considering all the model statistics, TLR + Dr was found to be the parameterization that best simulated observed GPP and LE and was therefore chosen to study the impacts of future changes in SWC and O_3 on plant productivity and gas exchange.

3.2 | Future impacts of drought and O_3 stress

To assess how closely FORCAsT was able to reproduce observed GPP and LE driven by meteorological and O_3 data from each GCM, a test simulation was conducted for each site using bias-corrected 'historical' data for the period 1996–2005 (Figure S2). Figure 4 shows that although there were differences in the GPP and LE estimated from each individual GCM, the ensemble means closely matched estimates made using observed meteorology. The good performance of the historical GCM driving data relative to the observed driving data is further confirmed by low RMSEs, high correlation coefficients and low *SD*s (see Taylor diagrams in Figure S6), lending confidence in our use of ensemble mean driving data for future simulations.

3.3 | Changes in GPP and LE in future

Figure 5 shows ensemble means of modelled estimates of GPP and LE using bias-corrected GCM data and TLR + Dr (the best model configuration) at each site for 2041–2050 and 2091–2100 as well as present-day estimates based on historical GCM and observed driving data. GPP and LE estimates for individual ensemble members for 2041–2050 and 2091–2100 are presented in Figures S9 and S10 and show that while there is general agreement about changes to mid-century, there is greater uncertainty towards the end of the century. They also show good agreement between ensemble members at the beginning of the year, but they begin to diverge during at the start of the growing season which also coincides with changes in SWC and O_3.

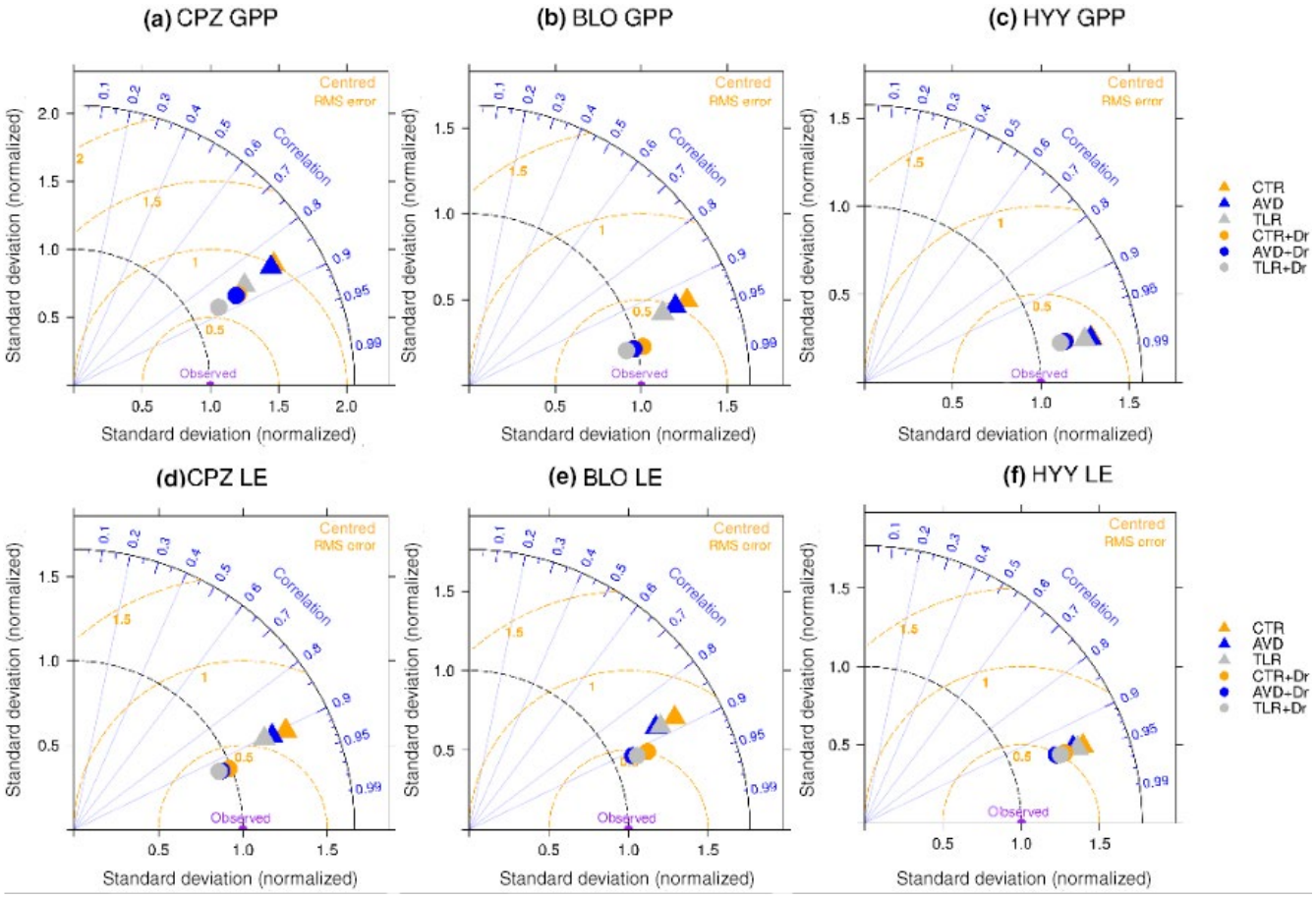

FIGURE 3 Taylor diagram showing model output statistics from FORCAsT simulations. Panels a, b and c show output statistics for gross primary productivity (GPP) at CPZ, BLO and HYY respectively while panels d, e and f show output statistics for latent heat flux (LE) at the same sites. Black and orange dashed curves and blue lines show normalized standard deviation (*SD*), centred root mean squared error (RMSE) and correlation coefficients (*r*) respectively against observations. Observed GPP and LE have *SD* = 1.0, RMSE = 0.0 and *r* = 1.0 (purple circle). The summary statistics for each model simulation are shown by orange (CTR and CTR + Dr), blue (AVD and AVD + Dr), and grey (TLR and TLR + Dr). Triangles represent simulations without drought stress and circles those with. Note the difference in scale of standard deviation on panel (a)

GPP is projected to increase by the middle and end of the 21st century at all three sites (Figure 5). Relative to present-day estimates, GPP could increase by 7% at CPZ (from 150 to 161 g C m^{-2} $year^{-1}$), 5% at BLO (from 151 to 158 g C m^{-2} $year^{-1}$) and 8% at HYY (from 90 to 96 g C m^{-2} $year^{-1}$) by 2041–2050 while LE is projected to increase by 10%, 2% and 9% for the same period. By 2091–2100, GPP could increase by 14% at CPZ and HYY and 11% at BLO while LE increases at CPZ and HYY by 13% and 10% relative to present-day estimates but decreases by 4% at BLO. For CPZ and BLO, these projected increases in GPP and LE occur throughout the year, but at HYY, the increase starts in spring. However, as shown by Figures S9 and S10, there is uncertainty about the projected GPP and LE fluxes in future as individual GCM ensemble members provide diverse estimates. The uncertainty is higher between 2091 and 2100 (Figure S10) than 2041–2050 (Figure S9). The projected decrease in ensemble mean LE at BLO is due to lower LE estimated by several individual GCM ensemble members as shown on Figure S9. HYY and CPZ are expected to experience higher percentage increases in productivity between the middle and end of the century than BLO although the overall productivity level at HYY will remain lower than those at CPZ and BLO. The higher productivity projected for CPZ and HYY could be due to bigger increase in projected winter and spring temperatures at the two sites (Figures S3 and S4), which is likely to extend the length of the growing season at these sites.

3.4 | Impacts of drought and O_3 through the 21st century

Figure 6 shows the impact of drought and O_3 stress on future GPP and LE fluxes by mid-century (2041–2050) and end of century (2091–2100). As for present-day simulations, modelled GPP and LE at all three sites were highest when neither the effects of drought or O_3 stress were included. Modelled GPP and LE were lowest when both were included (FUT + DrO_3), with the impact of drought stress (FUT + Dr) again far outweighing that of O_3 (FUT + O_3).

The impact of drought stress on modelled GPP and LE flux increases through the century. As shown in Figure 6, drought stress has

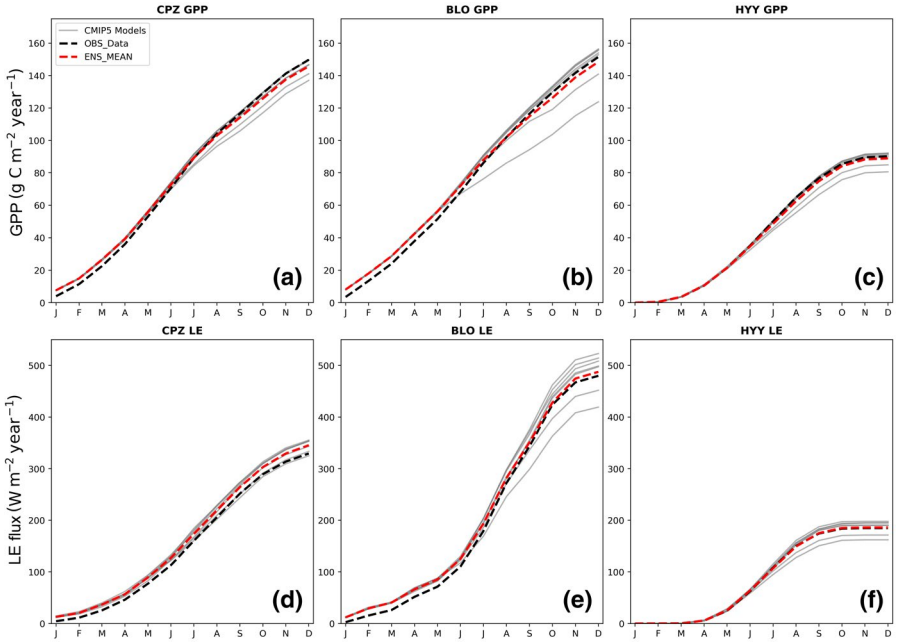

FIGURE 4 Estimates of gross primary productivity (GPP; a–f) and latent heat flux (LE; d–e) at CPZ, BLO and HYY respectively using bias-corrected historical (1996–2005) general circulation model (GCM) output data compared with estimates from observed driving data. Ensemble mean is indicated by red dashed lines while present-day estimates are shown in black dashed lines. Individual GCM estimates are shown by grey lines

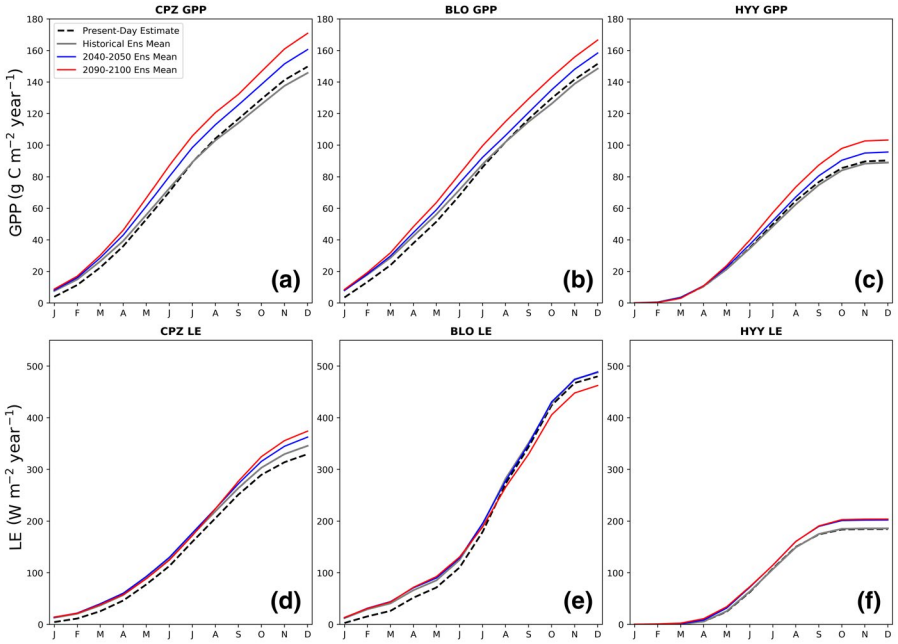

FIGURE 5 Ensemble mean estimates of average yearly gross primary productivity (GPP) (a–c) and latent heat flux (LE) (d–f) compared with present-day estimates using observed driving data for CPZ, BLO and HYY respectively. Ensemble means for 2041–2050 and 2091–2100 are indicated by blue and red lines respectively while present-day estimates are shown by grey lines (historical general circulation model driving data) and black dashed lines (observed driving data)

a higher impact on estimated LE than GPP at all three sites between 2041 and 2050, but this is reversed towards the end of the century as drought stress leads to a greater reduction on GPP than LE at CPZ and BLO and has similar impacts on GPP and LE at HYY between 2091 and 2100. For both periods, drought stress is projected to have higher impacts at the Mediterranean forests than the Boreal forest. This is similar to present-day simulations and indicates that the relative impacts of drought stress in different climatic regions are unlikely to change. For instance, drought stress causes a reduction of 21% and 19% in GPP and LE, respectively, at CPZ between 2091 and 2100 compared to 16% and 18% between 2041 and 2050. Similarly, at BLO, GPP and LE are reduced by 18% and 17%, respectively, in 2091–2100 compared to a projected decrease of 14% and 16% by mid-century. There is negligible difference between the impacts of drought stress on either GPP or LE at the end and middle of the century at HYY.

The addition of O_3 stress based on the tolerance parameterization (FUT + O_3) reduced estimated GPP and LE at all three sites compared to FUT, although the reduction was more pronounced at CPZ and BLO than at HYY and for 2041–2050 than 2091–2100. GPP could be reduced by 3%–4% due to O_3 damage by mid-century but only 2%–3% (1% less) by the end of the century, with similar impacts seen on LE across all sites.

Figure 6 shows that the combined effect of drought and O_3 stress leads to bigger decreases, but there are differences in the

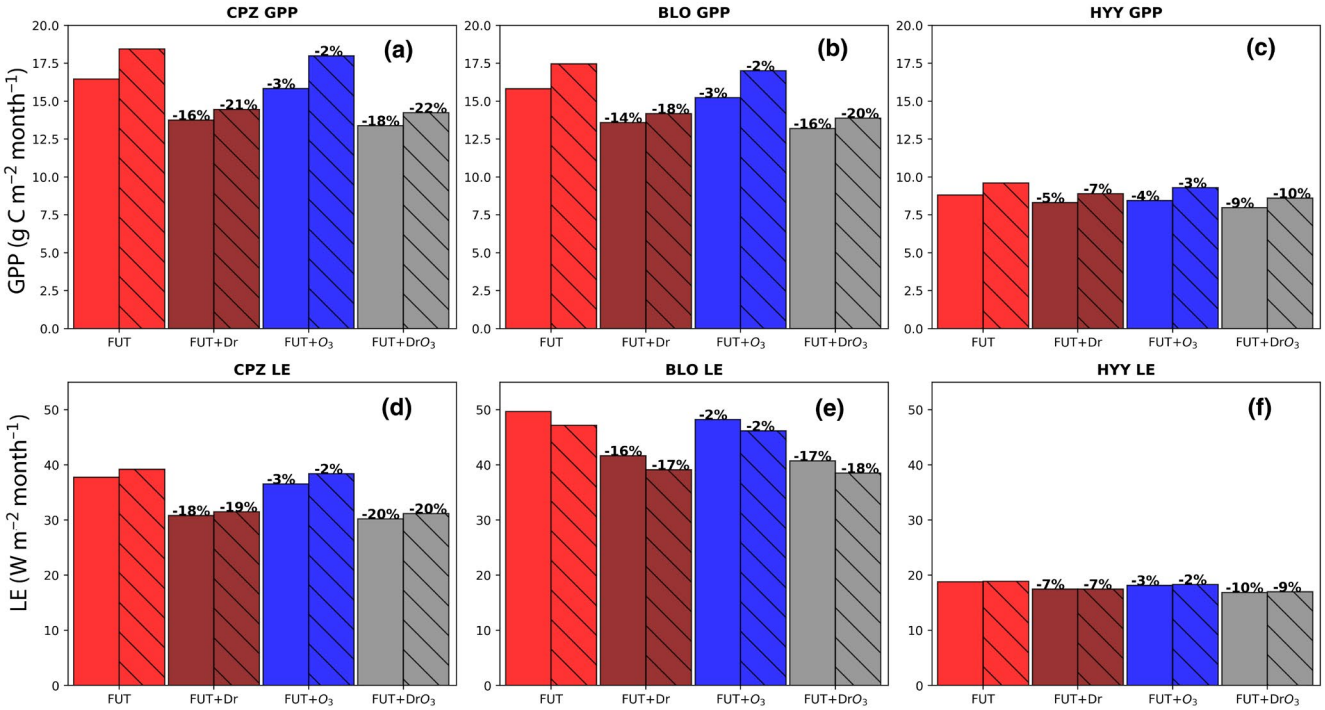

FIGURE 6 CMIP5 ensemble mean estimates of gross primary productivity (GPP) and latent heat flux (LE) for the period 2041–2050 (plain bars) and 2091–2100 (striped bars). Panels (a–c) show GPP and (d–f) LE for Castelporziano (CPZ), Blodgett (BLO) and Hyytiälä (HYY) respectively. Red, brown, blue and grey bars represent FUT, FUT + Dr, FUT + O_3 and FUT + DrO_3 model simulations respectively

impacts at each site and during different periods. For example, the combined impact of drought and O_3 stress is higher at CPZ and BLO than HYY reflecting the projected changes in SWC and O_3 mixing ratios at these sites (shown in Figures S3 and S4). By mid-century, drought and O_3 stress could lead to reductions in GPP and LE at CPZ from 16 to 13 g C m^{-2} month^{-1} and 38–30 W m^{-2} month^{-1}, decreases of 18% and 20% respectively. The combined impact of drought and O_3 stress on GPP increases to a reduction of ~22% by the end of the century, although their impact on LE remains unchanged. Reductions in GPP and LE are also projected for BLO and HYY as shown on Figure 6.

For the Mediterranean sites, there is a marginal difference (~1% lower) between the sum of drought and O_3 impacts on GPP and LE when applied separately than when the two stressors are applied together while no difference is observed at HYY. This is smaller than the 5% difference seen under present-day conditions, which suggested that the two stresses interact and could compensate for each other.

4 | DISCUSSION

We investigated the current and future impacts of drought and O_3 stress on gas exchange and forest productivity in three NH forests: Mediterranean forests at BLO and CPZ and a Boreal forest at HYY. We found that all three become more productive over time with GPP projected to increase by 7%, 5% and 8% at CPZ, BLO and HYY by 2041–2050 and by 14%, 11% and 14% by 2091–2100, in line with previous studies. For example, Madani et al. (2018) found a 31% increase in GPP for the NH under the RCP8.5 scenario by 2070, similar to the increases of 36%, 31% and 24% at CPZ, BLO and HYY, respectively, we see by 2100 in the absence of drought and O_3, though it must be noted that the increase estimated by Madani et al. (2018) is averaged over mid and high latitudes of the entire NH (>45°N), rather than for individual sites.

Under RCP8.5, CO_2 concentrations are projected to increase rapidly from current values of ~380 to 936 ppm by 2100, and average global temperature by 4.5°C with some areas experiencing even higher temperature increases as shown by Figures S3 and S4. Warmer temperatures could lead to an earlier onset of the growing season (Menzel et al., 2006) leading to increased plant productivity early in the season (Keenan, Chin, & Whorf, 2014). Increased atmospheric CO_2 is also expected to provide additional atmospheric CO_2 for photosynthesis, and the resultant CO_2 fertilization (a phenomenon observed in FACE experiments; e.g. Norby, Warren, Iversen, Medlyn, & McMurtrie, 2010) drives the modelled increase in productivity. The effect of both increased global temperatures and CO_2 fertilization has been accounted for in this study through the use of bias-corrected CMIP5 data to drive FORCAsT.

We found increases in plant productivity at all study sites which could be explained by CO2 fertilization effect and the impact of warmer global temperatures. Increased productivity suggests an increased carbon sequestration capability by these forests, but such an interpretation is limited by several factors. For instance, Jiang et al. (2020) and Norby et al. (2010) have shown that although mature trees can take up more CO_2 under elevated conditions, assimilation is ultimately limited by the availability of other nutrients with

re-emission of the extra carbon back into the atmosphere observed. Nitrogen (Norby et al., 2010) and phosphorus (Cleveland et al., 2013) availability are particularly crucial to terrestrial carbon storage as they regulate plant productivity throughout the terrestrial biosphere (Cleveland et al., 2013). Wieder, Cleveland, Smith, and Todd-Brown (2015) have shown that accounting for nitrogen and nitrogen–phosphorus limitation could lower model-projected primary productivity substantially, highlighting the important role that these two nutrients could play in the ability of plants to sequester CO_2 in future. However, it is not currently understood how soil nutrient availability will change in future and we have not explicitly considered that here.

Plant response to increasing atmospheric CO_2 is also modulated by drought and temperature (Gray et al., 2016; Manderscheid, Erbs, & Weigel, 2014), factors which could become even more relevant in the warmer drier climate projected under RCP8.5. Other factors that could limit the CO_2 fertilization effect in forests include tree species migration (Midgley, Thuiller, & Higgins, 2007; Scheller & Mladenoff, 2005) and forest management practices which could affect the structure, density and tree diversity in these forests, and hence the impacts estimated here. Therefore, our simulations are intended to investigate specific ecosystems (three managed forests) and do not attempt to predict responses for broad PFTs. By using driving data from a range of GCMs, the impact of future changes in drought and temperature and their associated uncertainties have been implicitly accounted for in our estimate of changes in GPP and LE. However, we have not explored the impacts of the availability of soil nutrients or tree age on future GPP and LE. This presents an uncertainty in the projected increases in plant productivity for middle and end of the century and the impact these will have on carbon uptake at the study sites.

Unique to this study, we have tested how plant responses to O_3 exposure (i.e. tolerance or avoidance) affect model estimates of GPP and LE at each site. We found that the assumption that plants tolerate O_3 stress by reducing the subsequent internal damage was better at explaining the observed GPP at all sites while avoidance of O_3 appeared better suited to LE. However, this difference likely arises from the parameterization approach taken in each case. Under the tolerance approach following Sitch et al. (2007), we assumed that photosynthesis and stomatal conductance (g_s) are downregulated equally in response to increasing stomatal O_3 flux. However, our results suggest that O_3 stress affects A and gs with different intensity, inducing a decoupling effect between the two processes as described by Lombardozzi, Levis, Bonan, Hess, and Sparks (2015). Therefore, the application of a correction factor derived from the response of *A* to O_3 uptake (as in Equation 10) led to an underestimation of the impact of O_3 on gs and consequently LE. The avoidance method (Hoshika, Watanabe, et al., 2013) assumes that only g_s is directly affected as stomatal O_3 flux increases, with only an indirect impact on photosynthetic rate. Plant transpiration rates, and hence LE, however, are controlled only by gs, resulting in a greater impact on LE.

When comparing the O_3 stress strategies alone (when drought stress function β was set to 1), we observed that the best performances were provided by applying the tolerance strategy in the study sites characterized by a Mediterranean climate. We hypothesize that in these sites, drought-induced stomatal control dominates over the O_3-induced stomatal control protecting plants from both the stressors (Löw et al., 2006) and that their characteristic O_3-induced antioxidants production (Nali et al., 2004; Paoletti, 2006) was best accounted for by the tolerance strategy. Conversely in Hyytiala, where drought stress is less pronounced, the O_3-induced stomatal control could be more relevant, explaining the better performance of the avoidance strategy at this site.

Our findings that the assumption of tolerance provided a better model-observation fit for GPP while avoidance appeared more appropriate for LE suggests that stomatal and stomatal limitations to plant productivity and gas exchange under O_3 exposure are similar to that found under drought stress (e.g. De Kauwe et al., 2015; Egea et al., 2011; Keenan et al., 2010). However, as demonstrated in this study, such limitations are dependent on climatic conditions and tree or crop species. Future modelling and laboratory studies are required, focused on developing parameterization schemes to enable estimation of the combined effect of stomatal and non-stomatal O_3 damage and to improve the quantification of O_3 uptake by plants and its impact on plant and crop productivity.

Unsurprisingly, our simulations suggest that O_3 stress will become less important between the middle and end of the century at all the study sites. There could be several possible explanations for the decreasing impacts of O_3 in future. First, the RCP8.5 scenario assumes an increase in atmospheric CO_2 concentration from ~390 to 936 ppm by 2100 (IPCC, 2014), which would reduce stomatal conductance (e.g. Mills, Hayes, et al., 2011; Mills, Pleijel, et al., 2011), the key determinant of stomatal O_3 flux (Emberson et al., 2018). Elevated CO_2 has been observed to significantly decrease O_3 damage in several plant species (Fiscus, Reid, Miller, & Heagle, 1997; Harmens, Mills, Emberson, & Ashmore, 2007; Mills, Hayes, et al., 2011; Mills, Pleijel, et al., 2011). Our results show a decrease in stomatal conductance in future relative to the present day which is likely to reduce stomatal O_3 flux and hence its impact. Second, the decreasing impact of O_3 on plants could also be due to the interactive effects of drought and O_3 stress on plants as drought stress reduces stomatal conductance (e.g. Basu et al., 2016; Farooq et al., 2009). In FORCAsT, as most coupled stomatal conductance–photosynthesis models, drought stress directly downregulates both stomatal conductance and photosynthesis rates (e.g. Clark et al., 2011; De Kauwe et al., 2015; Egea et al., 2011; Keenan et al., 2010). In present-day simulations, we found that the combined effects of the two stresses were up to 5% lower than the sum of the impacts of the two stresses acting individually. A similar but less pronounced interaction between the two stresses is also seen in future simulations (Figure 6). We therefore conclude that the decreasing impacts of O_3 stress in future climates are partly due to the decrease in stomatal conductance as a result of increasing frequency and severity in drought stress projected for future climates (Dai, 2011; IPCC, 2014). This conclusion is supported by recent findings that future stomatal O_3 uptake in plants will decrease under drought stress (e.g. see Fuhrer, 2009; Lin et al., 2020).

We found that drought stress had a greater effect on estimated GPP and LE than O_3 stress at all sites across all time periods and

was more pronounced at the Mediterranean sites (CPZ and BLO). We hypothesized that when water availability is limited, Mediterranean vegetation is more responsive to drought stress than to O_3 exposure (Löw et al., 2006), so stomatal regulation induced by drought stress indirectly acts as O_3 response, by reducing the O_3 stomatal flux together with the water loss, explaining also the reduced predictive ability of the model when both stressors are combined (Figure 6). Although a general rapid reduction of stomatal aperture in response to short-term exposure to O_3 was observed (Wittig et al., 2007), the chronic exposure to O_3 may induce a phenomenon known as 'stomatal sluggishness', that is, a reduction of plant's ability to regulate stomata (Carriero et al., 2015; Emberson et al., 2009; Hoshika, De Marco, Materassi, & Paoletti, 2015; Hoshika et al., 2016; Hoshika, Watanabe, Carrari, Paoletti, & Koike., 2018). This is a serious problem for plants, since it can lead to plants inability to regulate the loss of water (Paoletti, 2005; Sun et al., 2012) further exacerbating the impacts of other stresses such as drought. O_3-induced stomatal sluggishness could therefore magnify the higher impact of drought on GPP and LE at the sites with Mediterranean climate, where O_3 concentrations are high relative to the Boreal site (HYY). However, there is not previous clear scientific evidence of sluggishness on sclerophyll leaves (i.e. *Q. ilex*) or Pine needles (i.e. *P. ponderosa*), and we did not explicitly account for sluggishness in this study. We believe that long-term O_3 fumigation experiments are needed to identify species-specific response of A and g_s to O_3 including sluggishness effects.

In present-day simulations, the inclusion of drought stress alone led to ~20% decrease in estimated GPP and LE at CPZ and BLO, but at HYY, the reduction was only 13% for GPP and 10% for LE. This is a surprising result considering that drought is an annual occurrence at CPZ and BLO, and accounting for drought stress has been shown to improve model fit to observations of photosynthesis in Mediterranean ecosystems (Fares et al., 2019; Keenan et al., 2010). This indicates that although plants in Mediterranean ecosystems have adapted to drought stress (Calfapietra et al., 2009; Paoletti, 2006), their growth and productivity is still likely to be negatively impacted by any further decrease in SWC. The results for HYY over the 1997–2014 period (Figure S5) and 2005–2006 (Figures 2 and 3), and observed effects in Boreal forests in Canada (Kljun, Sabate, & Gracia, 2007; Krishnan, 2006), Finland (Gao et al., 2016) and across Europe (Ciais et al., 2005) show that even for a well-watered forest, anomalous drought events can have a big impact on plant productivity. The Boreal region, extending across North America, Europe and Asia, constitutes the second largest forested biome after tropical forests (Landsberg & Gower, 1997) and therefore plays an important role in the global carbon cycle (Keeling, Chin, & Whorf, 1996). As global climate changes, productivity in Boreal ecosystems will be at a risk from drought stress although this effect could be mitigated by longer growing seasons which would potentially increase productivity as has been seen in other regions (e.g. Dragoni et al., 2011; White, Running, & Thornton, 1999).

One of the main challenges hindering accurate quantification of drought and O_3 stress impacts is the lack of long-term measurements at an appropriate spatial and temporal resolution for model parameterization, calibration and evaluation (see review by Emberson et al., 2018). In this study, we use half-hourly measurements of SWC and O_3 and empirical equations that relate these stresses to plant productivity and gas exchange. Present-day simulations show that incorporating both drought and O_3 stress gives the best model fit to observed GPP and LE, and that these two stresses counteract each other. Productivity increases in our Mediterranean and Boreal forest sites, with GPP (and potentially carbon sequestration) increasing by between 11% and 14%. Although we have not investigated future changes for other ecosystems, if our results were scaled to the regional level, the projected increase in GPP could be significant for the global carbon budget.

ACKNOWLEDGEMENTS

F.O.-L. is grateful to the Faculty of Science and Technology (FST) and Lancaster Environment Centre (LEC) at Lancaster University for funding his PhD Studentship. K.A. is a Royal Society Dorothy Hodgkin Fellow and thanks the Royal Society of London for their support and funding (DH150070). The authors are grateful to SMEAR II for the provision of O_3 data for HYY, to the General Secretariat of the Presidency of Italian Republic for supporting the research at CPZ, and Prof. Allen Goldstein for coordination of research at the BLO site. We are also grateful to FLUXNET for the provision of model input and evaluation data through the FLUXNET 2015 Dataset. Finally, we would like to thank Paul Young of Lancaster Environment Centre for providing quality controlled CMIP5 O_3 data used in this study.

CONFLICT OF INTEREST

The authors declare no conflict of interest.

AUTHOR CONTRIBUTION

All authors designed the experiment and contributed to writing the manuscript. F.O.-L. and K.A. carried out the modelling work and analysed the output data.

DATA AVAILABILITY STATEMENT

FLUXNET-2015 data can be downloaded from https://fluxnet.fluxdata.org/data/fluxnet2015-dataset.

O_3 data for HYY can be downloaded from https://avaa.tdata.fi/web/smart/smear/download.

O_3 data for CPZ and BLO, and the FORCAsT code are available on request to the corresponding authors.

ORCID

Frederick Otu-Larbi https://orcid.org/0000-0001-6991-1871
Kirsti Ashworth https://orcid.org/0000-0001-5627-3014

REFERENCES

Ainsworth, E. A., Yendrek, C. R., Sitch, S., Collins, W. J., & Emberson, L. D. (2012). The effects of tropospheric O_3 on net primary

productivity and implications for climate change. *Annual Review of Plant Biology*, *63*, 637–661. https://doi.org/10.1146/annurev-arplant-042110-103829

Andersen, C. P. (2003). Source–sink balance and carbon allocation below ground in plants exposed to O_3. *New Phytologist*, *157*(2), 213–228. https://doi.org/10.1046/j.1469-8137.2003.00674.x

Ashmore, M. R. (2005). Assessing the future global impacts of O_3 on vegetation. *Plant, Cell & Environment*, *28*(8), 949–964. https://doi.org/10.1111/j.1365-3040.2005.01341.x

Ashworth, K., Chung, S. H., Griffin, R. J., Chen, J., Forkel, R., Bryan, A. M., & Steiner, A. L. (2015). FORest Canopy Atmosphere Transfer (FORCAsT) 1.0: A 1-D model of biosphere–atmosphere chemical exchange. *Geoscientific Model Development*, *8*(11), 3765–3784. https://doi.org/10.5194/gmd-8-3765-2015

Ashworth, K., Chung, S. H., McKinney, K. A., Liu, Y., Munger, J. W., Martin, S. T., & Steiner, A. L. (2016). Modelling bidirectional fluxes of methanol and acetaldehyde with the FORCAsT canopy exchange model. *Atmospheric Chemistry and Physics*, *16*(24), https://doi.org/10.5194/acp-16-15461-2016

Basu, S., Ramegowda, V., Kumar, A., & Pereira, A. (2016). Plant adaptation to drought stress. *F1000Research*, *5*. https://doi.org/10.12688/f1000research.7678.1

Bréda, N., Cochard, H., Dreyer, E., & Granier, A. (1993). Field comparison of transpiration, stomatal conductance and vulnerability to cavitation of *Quercus petraea* and *Quercus robur* under water stress. *Annales Des Sciences Forestières*, *50*(6), 571–582. https://doi.org/10.1051/forest:19930606

Bryan, A. M., Bertman, S. B., Carroll, M. A., Dusanter, S., Edwards, G. D., Forkel, R., … Steiner, A. L. (2012). In-canopy gas-phase chemistry during CABINEX 2009: Sensitivity of a 1-D canopy model to vertical mixing and isoprene chemistry. *Atmospheric Chemistry and Physics*, *12*(18), 8829–8849. https://doi.org/10.5194/acp-12-8829-2012

Bryan, A. M., Cheng, S. J., Ashworth, K., Guenther, A. B., Hardiman, B. S., Bohrer, G., & Steiner, A. L. (2015). Forest-atmosphere BVOC exchange in diverse and structurally complex canopies: 1-D modeling of a mid-successional forest in northern Michigan. *Atmospheric Environment*, *120*, 217–226. https://doi.org/10.1016/j.atmosenv.2015.08.094

Büker, P., Feng, Z., Uddling, J., Briolat, A., Alonso, R., Braun, S., … Marzuoli, R. (2015). New flux based dose–response relationships for O_3 for European forest tree species. *Environmental Pollution*, *206*, 163–174. https://doi.org/10.1016/j.envpol.2015.06.033

Calfapietra, C., Fares, S., & Loreto, F. (2009). Volatile organic compounds from Italian vegetation and their interaction with O_3. *Environmental Pollution*, *157*(5), 1478–1486. https://doi.org/10.1016/j.envpol.2008.09.048

Carriero, G., Emiliani, G., Giovannelli, A., Hoshika, Y., Manning, W. J., Traversi, M. L., & Paoletti, E. (2015). Effects of long-term ambient ozone exposure on biomass and wood traits in poplar treated with ethylenediurea (EDU). *Environmental Pollution*, *206*, 575–581. https://doi.org/10.1016/j.envpol.2015.08.014

Chevone, B. (1991). Seasonal changes in components of the antioxidant system in eastern white pine and ozone effects on antioxidant metabolism. *Air & Waste Management Association*, 91–142.

Ciais, P. H., Reichstein, M., Viovy, N., Granier, A., Ogée, J., Allard, V., … Valentini, R. (2005). Europe-wide reduction in primary productivity caused by the heat and drought in 2003. *Nature*, *437*(7058), 529–533. https://doi.org/10.1038/nature03972

Clark, D. B., Mercado, L. M., Sitch, S., Jones, C. D., Gedney, N., Best, M. J., … Cox, P. M. (2011). The Joint UK Land Environment Simulator (JULES), model description – Part 2: Carbon fluxes and vegetation dynamics. *Geoscientific Model Development*, *4*(3), 701–722. https://doi.org/10.5194/gmd-4-701-2011

Clenciala, E., Kucera, J., Ryan, M. G., & Lindroth, A. (1998). Water flux in boreal forest during two hydrologically contrasting years; species specific regulation of canopy conductance and transpiration. *Annales Des Sciences Forestières*, *55*(1-2), 47–61. https://doi.org/10.1051/forest:19980104

Cleveland, C. C., Houlton, B. Z., Smith, W. K., Marklein, A. R., Reed, S. C., Parton, W., … Running, S. W. (2013). Patterns of new versus recycled primary production in the terrestrial biosphere. *Proceedings of the National Academy of Sciences of the United States of America*, *110*(31), 12733–12737. https://doi.org/10.1073/pnas.1302768110

Dai, A. (2011). Drought under global warming: A review. *Wiley Interdisciplinary Reviews: Climate Change*, *2*(1), 45–65. https://doi.org/10.1002/wcc.81

De Kauwe, M. G., Kala, J., Lin, Y.-S., Pitman, A. J., Medlyn, B. E., Duursma, R. A., … Miralles, D. G. (2015). A test of an optimal stomatal conductance scheme within the CABLE land surface model. *Geoscientific Model Development*, *8*(2), 431–452. https://doi.org/10.5194/gmd-8-431-2015

De Marco, A., Sicard, P., Fares, S., Tuovinen, J. P., Anav, A., & Paoletti, E. (2016). Assessing the role of soil water limitation in determining the Phytotoxic Ozone Dose (PODY) thresholds. *Atmospheric Environment*, *147*, 88–97. https://doi.org/10.1016/j.atmosenv.2016.09.066

Dragoni, D., Schmid, H. P., Wayson, C. A., Potter, H., Grimmond, C. S. B., & Randolph, J. C. (2011). Evidence of increased net ecosystem productivity associated with a longer vegetated season in a deciduous forest in south-central Indiana, USA. *Global Change Biology*, *17*(2), 886–897. https://doi.org/10.1111/j.1365-2486.2010.02281.x

Egea, G., Verhoef, A., & Vidale, P. L. (2011). Towards an improved and more flexible representation of water stress in coupled photosynthesis–stomatal conductance models. *Agricultural and Forest Meteorology*, *151*(10), 1370–1384. https://doi.org/10.1016/j.agrformet.2011.05.019

Emberson, L. D., Ashmore, M. R., Cambridge, H. M., Simpson, D., & Tuovinen, J. P. (2000). Modelling stomatal O_3 flux across Europe. *Environmental Pollution*, *109*(3), 403–413. https://doi.org/10.1016/S0269-7491(00)00043-9

Emberson, L. D., Büker, P., & Ashmore, M. R. (2007). Assessing the risk caused by ground level ozone to European forest trees: A case study in pine, beech and oak across different climate regions. *Environmental Pollution*, *147*(3), 454–466. https://doi.org/10.1016/j.envpol.2006.10.026

Emberson, L. D., Büker, P., Ashmore, M. R., Mills, G., Jackson, L. S., Agrawal, M., … Wahid, A. (2009). A comparison of North American and Asian exposure–response data for ozone effects on crop yields. *Atmospheric Environment*, *43*(12), 1945–1953. https://doi.org/10.1016/j.atmosenv.2009.01.005

Emberson, L. D., Pleijel, H., Ainsworth, E. A., Van den Berg, M., Ren, W., Osborne, S., … Ewert, F. (2018). O_3 effects on crops and consideration in crop models. *European Journal of Agronomy*, *100*, 19–34. https://doi.org/10.1016/j.eja.2018.06.002

Fares, S., Alivernini, A., Conte, A., & Maggi, F. (2019). O_3 and particle fluxes in a Mediterranean forest predicted by the AIRTREE model. *Science of the Total Environment*, *682*, 494–504. https://doi.org/10.1016/j.scitotenv.2019.05.109

Farooq, M., Wahid, A., Kobayashi, N., Fujita, D. B. S. M. A., & Basra, S. M. A. (2009). Plant drought stress: Effects, mechanisms and management. *Sustainable agriculture* (pp. 153–188). Dordrecht: Springer. https://doi.org/10.1007/978-90-481-2666-8_12

Farquhar, G. D., Von Caemmerer, S., & Berry, J. A. (1980). A biochemical model of photosynthetic carbon dioxide assimilation in leaves of 3-carbon pathway species. *Planta*, *149*, 78–90.

Fiscus, E. L., Reid, C. D., Miller, J. E., & Heagle, A. S. (1997). Elevated CO_2 reduces O_3 flux and O_3-induced yield losses in soybeans: Possible implications for elevated CO_2 studies. *Journal of Experimental Botany*, *48*(2), 307–313. https://doi.org/10.1093/jxb/48.2.307

Fuhrer, J. (2009). O_3 risk for crops and pastures in present and future climates. *Naturwissenschaften*, *96*(2), 173–194. https://doi.org/10.1007/s00114-008-0468-7

Gao, Y., Markkanen, T., Thum, T., Aurela, M., Lohila, A., Mammarella, I., … Aalto, T. (2016). Assessing various drought indicators in representing summer drought in boreal forests in Finland. *Hydrology and Earth System Sciences*, *20*, 175–191. https://doi.org/10.5194/hess-20-175-2016

Gaudel, A., Cooper, R., Ancellet, G., Barret, B., Boynard, A., Burrows, J., … Doniki, S. (2018). Tropospheric ozone assessment report: Present-day distribution and trends of tropospheric ozone relevant to climate and global atmospheric chemistry model evaluation. *Elementa: Science of the Anthropocene*, *6*(1), art-39. https://doi.org/10.1525/elementa.291

Granier, A., Reichstein, M., Bréda, N., Janssens, I. A., Falge, E., Ciais, P., … Wang, Q. (2007). Evidence for soil water control on carbon and water dynamics in European forests during the extremely dry year: 2003. *Agricultural and Forest Meteorology*, *143*(1–2), 123–145. https://doi.org/10.1016/j.agrformet.2006.12.004

Gray, S. B., Dermody, O., Klein, S. P., Locke, A. M., McGrath, J. M., Paul, R. E., … Leakey, A. D. B. (2016). Intensifying drought eliminates the expected benefits of elevated carbon dioxide for soybean. *Nature Plants*, *2*(9), 1–8. https://doi.org/10.1038/nplants.2016.132

Grüters, U., Fangmeier, A., & Jäger, H. J. (1995). Modelling stomatal responses of spring wheat (*Triticum aestivum* L. cv. Turbo) to O_3 and different levels of water supply. *Environmental Pollution*, *87*(2), 141–149. https://doi.org/10.1016/0269-7491(94)P2600-E

Hari, P., & Kulmala, M. (2005). Station for Measuring Ecosystem Atmosphere Relations (SMEAR II). *Boreal Environmental Research*, *10*, 315–322.

Hari, P., Nikinmaa, E., Pohja, T., Siivola, E., Bäck, J., Vesala, T., & Kulmala, M. (2013). Station for measuring ecosystem-atmosphere relations: SMEAR. In P. Hari, K. Heliövaara, & L. Kulmala (Eds.), *Physical and physiological forest ecology*. Dordrecht: Springer. https://doi.org/10.1007/978-94-007-5603-8_9

Harmens, H., Mills, G., Emberson, L. D., & Ashmore, M. R. (2007). Implications of climate change for the stomatal flux of O_3: A case study for winter wheat. *Environmental Pollution*, *146*(3), 763–770. https://doi.org/10.1016/j.envpol.2006.05.018

Hartmann, D. L., Tank, A. M. K., Rusticucci, M., Alexander, L. V., Brönnimann, S., Charabi, Y. A. R., … Soden, B. J. (2013). Climate change 2013: Observations: Atmosphere and surface. In T. F. Stocker, D. Qin, G.-K. Plattner, M. Tignor, & S. K. Allen (Eds.), *Climate change 2013 the physical science basis: Working group I contribution to the fifth assessment report of the Intergovernmental Panel on Climate Change* (pp. 159–254). Cambridge University Press. Retrieved from www.climatechange2013.org and www.ipcc.ch

Hoshika, Y., De Marco, A., Materassi, A., & Paoletti, E. (2016). Light intensity affects ozone-induced stomatal sluggishness in snapbean. *Water, Air, & Soil Pollution*, *227*(11), 419. https://doi.org/10.1007/s11270-016-3127-1

Hoshika, Y., Katata, G., Deushi, M., Watanabe, M., Koike, T., & Paoletti, E. (2015). Ozone-induced stomatal sluggishness changes carbon and water balance of temperate deciduous forests. *Scientific Reports*, *5*, 9871. https://doi.org/10.1038/srep09871

Hoshika, Y., Omasa, K., & Paoletti, E. (2013). Both O_3 exposure and soil water stress are able to induce stomatal sluggishness. *Environmental and Experimental Botany*, *88*, 19–23. https://doi.org/10.1016/j.envexpbot.2011.12.004

Hoshika, Y., Watanabe, M., Carrari, E., Paoletti, E., & Koike, T. (2018). Ozone-induced stomatal sluggishness changes stomatal parameters of Jarvis-type model in white birch and deciduous oak. *Plant Biology*, *20*(1), 20–28. https://doi.org/10.1111/plb.12632

Hoshika, Y., Watanabe, M., Inada, N., & Koike, T. (2013). Model-based analysis of avoidance of O_3 stress by stomatal closure in Siebold's beech (*Fagus crenata*). *Annals of Botany*, *112*(6), 1149–1158. https://doi.org/10.1093/aob/mct166

IPCC [Intergovernmental Panel on Climate Change]. (2013). Near-term climate change: Projections and predictability. In T. F. Stocker, D. Qin, G.-K. Plattner, M. Tignor, S. K. Allen, J. Boschung, A. Nauels, Y. Xia, V. Bex, & P. M. Midgley (Eds.), *Climate change 2013: The physical science basis. Contribution of working group I to the fifth assessment report of the Intergovernmental Panel on Climate Change* (pp. 978–980). Cambridge, UK: Cambridge University Press.

IPCC [Intergovernmental Panel on Climate Change]. (2014). *Summary for policymakers. Climate change 2014: Impacts, adaptation and vulnerability – Contribution of working group II to fifth assessment report of the Intergovernmental Panel on Climate Change* (pp. 1–32). https://doi.org/10.1016/j.renene.2009.11.012

Jiang, M., Medlyn, B. E., Drake, J. E., Duursma, R. A., Anderson, I. C., Barton, C. V. M., … Ellsworth, D. S. (2020). The fate of carbon in a mature forest under carbon dioxide enrichment. *Nature*, *580*(7802), 227–231. https://doi.org/10.1038/s41586-020-2128-9

Kasischke, E. S. (2000). Boreal ecosystems in the global carbon cycle. In E. S. Kasischke & B. J. Stocks (Eds.), *Fire, climate change, and carbon cycling in the boreal forest* (pp. 19–30). New York, NY: Springer.

Keeling, C. D., Chin, J. F. S., & Whorf, T. P. (1996). Increased activity of northern vegetation inferred from atmospheric CO_2 measurements. *Nature*, *382*(6587), 146–149. https://doi.org/10.1038/382146a0

Keenan, T. F., Gray, J., Friedl, M. A., Toomey, M., Bohrer, G., Hollinger, D. Y., … Richardson, A. D. (2014). Net carbon uptake has increased through warming-induced changes in temperate forest phenology. *Nature Climate Change*, *4*(7), 598–604. https://doi.org/10.1038/nclimate2253

Keenan, T., Sabate, S., & Gracia, C. (2010). Soil water stress and coupled photosynthesis–conductance models: Bridging the gap between conflicting reports on the relative roles of stomatal, mesophyll conductance and biochemical limitations to photosynthesis. *Agricultural and Forest Meteorology*, *150*(3), 443–453. https://doi.org/10.1016/j.agrformet.2010.01.008

Kljun, N., Black, T. A., Griffis, T. J., Barr, A. G., Gaumont-Guay, D., Morgenstern, K., … Nesic, Z. (2007). Response of net ecosystem productivity of three boreal forest stands to drought. *Ecosystems*, *10*(6), 1039–1055. https://doi.org/10.1007/s10021-007-9088-x

Köppen, W. P. (1923). *Die klimate der erde: Grundriss der klimakunde*. Berlin, Germany: Walter de Gruyter GmbH & Co KG.

Krishnan, P., Black, T. A., Grant, N. J., Barr, A. G., Hogg, E. T. H., Jassal, R. S., & Morgenstern, K. (2006). Impact of changing soil moisture distribution on net ecosystem productivity of a boreal aspen forest during and following drought. *Agricultural and Forest Meteorology*, *139*(3–4), 208–223. https://doi.org/10.1016/j.agrformet.2006.07.002

Laisk, A., Kull, O., & Moldau, H. (1989). O_3 concentration in leaf intercellular air spaces is close to zero. *Plant Physiology*, *90*(3), 1163–1167. https://doi.org/10.1104/pp.90.3.1163

Landsberg, J. J., & Gower, S. T. (1997). *Applications of physiological ecology to forest management*. San Diego, CA: Academic Press.

Law, B. E., Kelliher, F. M., Baldocchi, D. D., Anthoni, P. M., Irvine, J., Moore, D. V., & Van Tuyl, S. (2001). Spatial and temporal variation in respiration in a young ponderosa pine forest during a summer drought. *Agricultural and Forest Meteorology*, *110*(1), 27–43. https://doi.org/10.1016/S0168-1923(01)00279-9

Leisner, C. P., & Ainsworth, E. A. (2012). Quantifying the effects of O_3 on plant reproductive growth and development. *Global Change Biology*, *18*(2), 606–616. https://doi.org/10.1111/j.1365-2486.2011.02535.x

Lhomme, J. P., Elguero, E., Chehbouni, A., & Boulet, G. (1998). Stomatal control of transpiration: Examination of Monteith's formulation of canopy resistance. *Water Resources Research*, *34*(9), 2301–2308. https://doi.org/10.1029/98WR01339

Lin, M., Horowitz, L. W., Xie, Y., Paulot, F., Malyshev, S., Shevliakova, E., … Pilegaard, K. (2020). Vegetation feedbacks during drought exacerbate O_3 air pollution extremes in Europe. *Nature Climate Change*, *10*(5), 444–451. https://doi.org/10.1038/s41558-020-0743-y

Lin, Y.-S., Medlyn, B. E., Duursma, R. A., Prentice, I. C., Wang, H., Baig, S., … Wingate, L. (2015). Optimal stomatal behaviour around the world.

Nature Climate Change, *5*(5), 459–464. https://doi.org/10.1038/nclimate2550

Lombardozzi, D., Levis, S., Bonan, G., Hess, P. G., & Sparks, J. P. (2015). The influence of chronic ozone exposure on global carbon and water cycles. *Journal of Climate*, *28*(1), 292–305. https://doi.org/10.1175/JCLI-D-14-00223.1

Löw, M., Herbinger, K., Nunn, A. J., Häberle, K.-H., Leuchner, M., Heerdt, C., … Matyssek, R. (2006). Extraordinary drought of 2003 overrules ozone impact on adult beech trees (*Fagus sylvatica*). *Trees*, *20*(5), 539–548. https://doi.org/10.1007/s00468-006-0069-z

Madani, N., Kimball, J. S., Ballantyne, A. P., Affleck, D. L. R., van Bodegom, P. M., Reich, P. B., … Running, S. W. (2018). Future global productivity will be affected by plant trait response to climate. *Scientific Reports*, *8*(1), 1–10. https://doi.org/10.1038/s41598-018-21172-9

Manderscheid, R., Erbs, M., & Weigel, H. J. (2014). Interactive effects of free-air CO_2 enrichment and drought stress on maize growth. *European Journal of Agronomy*, *52*, 11–21. https://doi.org/10.1016/j.eja.2011.12.007

Medlyn, B. E., Duursma, R. A., Eamus, D., Ellsworth, D. S., Prentice, I. C., Barton, C. V. M., … Wingate, L. (2011). Reconciling the optimal and empirical approaches to modelling stomatal conductance. *Global Change Biology*, *17*(6), 2134–2144. https://doi.org/10.1111/j.1365-2486.2010.02375.x

Menzel, A., Sparks, T. H., Estrella, N., Koch, E., Aasa, A., Ahas, R., … Zust, A. (2006). European phenological response to climate change matches the warming pattern. *Global Change Biology*, *12*(10), 1969–1976. https://doi.org/10.1111/j.1365-2486.2006.01193.x

M'Hirit, O. (1999). Mediterranean forests: Ecological space and economic and community wealth. *UNASYLVA*, FAO, 3–15.

Midgley, G. F., Thuiller, W., & Higgins, S. I. (2007). Plant species migration as a key uncertainty in predicting future impacts of climate change on ecosystems: Progress and challenges. *Terrestrial ecosystems in a changing world* (pp. 129–137). Berlin, Heidelberg: Springer. https://doi.org/10.1007/978-3-540-32730-1_11

Millán, M. M., Mantilla, E., Salvador, R., Carratalá, A., Sanz, M. J., Alonso, L., … Navazo, M. (2000). O_3 cycles in the western Mediterranean basin: Interpretation of monitoring data in complex coastal terrain. *Journal of Applied Meteorology*, *39*(4), 487–508. https://doi.org/10.1175/1520-0450(2000)039<0487:OCITWM>2.0.CO;2

Mills, G., Hayes, F., Simpson, D., Emberson, L., Norris, D., Harmens, H., & Büker, P. (2011). Evidence of widespread effects of O_3 on crops and (semi-) natural vegetation in Europe (1990–2006) in relation to AOT40- and flux-based risk maps. *Global Change Biology*, *17*(1), 592–613.

Mills, G., Pleijel, H., Braun, S., Büker, P., Bermejo, V., Calvo, E., … Simpson, D. (2011). New stomatal flux-based critical levels for ozone effects on vegetation. *Atmospheric Environment*, *45*(28), 5064–5068. https://doi.org/10.1016/j.atmosenv.2011.06.009

Nali, C., Paoletti, E., Marabottini, R., Della Rocca, G., Lorenzini, G., Paolacci, A. R., … Badiani, M. (2004). Ecophysiological and biochemical strategies of response to O_3 in Mediterranean evergreen broadleaf species. *Atmospheric Environment*, *38*(15), 2247–2257. https://doi.org/10.1016/j.atmosenv.2003.11.043

Nemani, R. R., Keeling, C. D., Hashimoto, H., Jolly, W. M., Piper, S. C., Tucker, C. J., … Running, S. W. (2003). Climate-driven increases in global terrestrial net primary production from 1982 to 1999. *Science*, *300*(5625), 1560–1563. https://doi.org/10.1126/science.1082750

Norby, R. J., Warren, J. M., Iversen, C. M., Medlyn, B. E., & McMurtrie, R. E. (2010). CO_2 enhancement of forest productivity constrained by limited nitrogen availability. *Proceedings of the National Academy of Sciences of the United States of America*, *107*(45), 19368–19373. https://doi.org/10.1073/pnas.1006463107

Omasa, K., & Takayama, K. (2002). Image instrumentation of chlorophyll a fluorescence for diagnosing photosynthetic injury. In *Air pollution and plant biotechnology* (pp. 287–308). Tokyo: Springer. https://doi.org/10.1007/978-4-431-68388-9_15

Osakabe, Y., Osakabe, K., Shinozaki, K., & Tran, L. S. P. (2014). Response of plants to water stress. *Frontiers in Plant Science*, *5*, 86. https://doi.org/10.3389/fpls.2014.00086

Otu-Larbi, F., Bolas, C. G., Ferracci, V., Staniaszek, Z., Jones, R. L., Malhi, Y., … Ashworth, K. (2020). Modelling the effect of the 2018 summer heatwave and drought on isoprene emissions in a UK woodland. *Global Change Biology*, *26*(4), 2320–2335. https://doi.org/10.1111/gcb.14963

Otu-Larbi, F., Conte, A., Fares, S., Williams, K., Wild, O., & Ashworth, K. (2020). FORCAsT2.0: Simulating photosynthesis and transpiration in a multi-layer forest canopy-atmosphere exchange model. (In preparation)

Panek, J. A., & Goldstein, A. H. (2001). Response of stomatal conductance to drought in ponderosa pine: Implications for carbon and O_3 uptake. *Tree Physiology*, *21*(5), 337–344. https://doi.org/10.1093/treephys/21.5.337

Paoletti, E. (2005). Ozone slows stomatal response to light and leaf wounding in a Mediterranean evergreen broadleaf, *Arbutus unedo*. *Environmental Pollution*, *134*(3), 439–445. https://doi.org/10.1016/j.envpol.2004.09.011

Paoletti, E. (2006). Impact of O_3 on Mediterranean forests: A review. *Environmental Pollution*, *144*(2), 463–474. https://doi.org/10.1016/j.envpol.2005.12.051

Paoletti, E. (2009). O_3 and Mediterranean ecology: Plants, people, problems. *Environmental Pollution*, *157*(5), 1397–1525.

Paoletti, E., & Grulke, N. E. (2010). O_3 exposure and stomatal sluggishness in different plant physiognomic classes. *Environmental Pollution*, *158*(8), 2664–2671. https://doi.org/10.1016/j.envpol.2010.04.024

Pastorello, G., Papale, D., Chu, H., Trotta, C., Agarwal, D., Canfora, E., … Torn, M. (2017). A new data set to keep a sharper eye on land-air exchanges. *Eos*, *Transactions American Geophysical Union*, *98*(8). https://doi.org/10.1029/2017EO071597

Pellegrini, E., Hoshika, Y., Dusart, N., Cotrozzi, L., Gérard, J., Nali, C., … Paoletti, E. (2019). Antioxidative responses of three oak species under ozone and water stress conditions. *Science of the Total Environment*, *647*, 390–399. https://doi.org/10.1016/j.scitotenv.2018.07.413

Pleijel, H., Danielsson, H., Ojanperä, K., De Temmerman, L., Högy, P., Badiani, M., & Karlsson, P. E. (2004). Relationships between O_3 exposure and yield loss in European wheat and potato – A comparison of concentration- and flux-based exposure indices. *Atmospheric Environment*, *38*(15), 2259–2269. https://doi.org/10.1016/j.atmosenv.2003.09.076

Riahi, K., Rao, S., Krey, V., Cho, C., Chirkov, V., Fischer, G., … Rafaj, P. (2011). RCP 8.5 – A scenario of comparatively high greenhouse gas emissions. *Climatic Change*, *109*(1–2), 33–57. https://doi.org/10.1007/s10584-011-0149-y

Scheller, R. M., & Mladenoff, D. J. (2005). A spatially interactive simulation of climate change, harvesting, wind, and tree species migration and projected changes to forest composition and biomass in northern Wisconsin, USA. *Global Change Biology*, *11*(2), 307–321. https://doi.org/10.1111/j.1365-2486.2005.00906.x

Sitch, S., Cox, P. M., Collins, W. J., & Huntingford, C. (2007). Indirect radiative forcing of climate change through O_3 effects on the land-carbon sink. *Nature*, *448*(7155), 791–794. https://doi.org/10.1038/nature06059

Sorooshian, S., Li, J., Hsu, K. L., & Gao, X. (2012). Influence of irrigation schemes used in regional climate models on evapotranspiration estimation: Results and comparative studies from California's Central Valley agricultural regions. *Journal of Geophysical Research: Atmospheres*, *117*(D6). https://doi.org/10.1029/2011JD016978

Sun, G. E., McLaughlin, S. B., Porter, J. H., Uddling, J., Mulholland, P. J., Adams, M. B., & Pederson, N. (2012). Interactive influences of ozone and climate on streamflow of forested watersheds. *Global Change Biology*, *18*(11), 3395–3409. https://doi.org/10.1111/j.1365-2486.2012.02787.x

Taylor, K. E. (2001). Summarizing multiple aspects of model performance in a single diagram. *Journal of Geophysical Research: Atmospheres*, *106*(D7), 7183–7192. https://doi.org/10.1029/2000JD900719

Taylor, K. E., Stouffer, R. J., & Meehl, G. A. (2012). An overview of CMIP5 and the experiment design. *Bulletin of the American Meteorological Society*, *93*(4), 485–498. https://doi.org/10.1175/BAMS-D-11-00094.1

White, M. A., Running, S. W., & Thornton, P. E. (1999). The impact of growing-season length variability on carbon assimilation and evapotranspiration over 88 years in the eastern US deciduous forest. *International Journal of Biometeorology*, *42*(3), 139–145. https://doi.org/10.1007/s004840050097

Wieder, W. R., Cleveland, C. C., Smith, W. K., & Todd-Brown, K. (2015). Future productivity and carbon storage limited by terrestrial nutrient availability. *Nature Geoscience*, *8*(6), 441–444. https://doi.org/10.1038/ngeo2413

Wilkinson, S., & Davies, W. J. (2010). Drought, O_3, ABA and ethylene: New insights from cell to plant to community. *Plant, Cell & Environment*, *33*(4), 510–525.

Wittig, V. E., Ainsworth, E. A., & Long, S. P. (2007). To what extent do current and projected increases in surface ozone affect photosynthesis and stomatal conductance of trees? A meta-analytic review of the last 3 decades of experiments. *Plant, Cell & Environment*, *30*(9), 1150–1162. https://doi.org/10.1111/j.1365-3040.2007.01717.x

Wittig, V. E., Ainsworth, E. A., Naidu, S. L., Karnosky, D. F., & Long, S. P. (2009). Quantifying the impact of current and future tropospheric O_3 on tree biomass, growth, physiology and biochemistry: A quantitative meta-analysis. *Global Change Biology*, *15*(2), 396–424. https://doi.org/10.1111/j.1365-2486.2008.01774.x

Yeung, L. Y., Murray, L. T., Martinerie, P., Witrant, E., Hu, H., Banerjee, A., … Chappellaz, J. (2019). Isotopic constraint on the twentieth-century increase in tropospheric O_3. *Nature*, *570*(7760), 224–227. https://doi.org/10.1038/s41586-019-1277-1

Young, P. J., Archibald, A. T., Bowman, K. W., Lamarque, J. F., Naik, V., Stevenson, D. S., … Zeng, G. (2013). Pre-industrial to end 21st century projections of tropospheric O_3 from the Atmospheric Chemistry and Climate Model Intercomparison Project (ACCMIP). *Atmospheric Chemistry and Physics*, *13*, 2063–2090. https://doi.org/10.5194/acp-13-2063-2013

Zhao, T., & Dai, A. (2017). Uncertainties in historical changes and future projections of drought. Part II: Model-simulated historical and future drought changes. *Climatic Change*, *144*(3), 535–548. https://doi.org/10.1007/s10584-016-1742-x.

Zhou, P., Ganzeveld, L., Rannik, Ü., Zhou, L., Gierens, R., Taipale, D., … Boy, M. (2017). Simulating O_3 dry deposition at a boreal forest with a multi-layer canopy deposition model. *Atmospheric Chemistry & Physics*, *17*(2). https://doi.org/10.5194/acp-17-1361-2017

Zhou, S., Medlyn, B., Sabaté, S., Sperlich, D., & Prentice, I. C. (2014). Short-term water stress impacts on stomatal, mesophyll and biochemical limitations to photosynthesis differ consistently among tree species from contrasting climates. *Tree Physiology*, *34*(10), 1035–1046. https://doi.org/10.1093/treephys/tpu072

SUPPORTING INFORMATION

Additional supporting information may be found online in the Supporting Information section.

How to cite this article: Otu-Larbi F, Conte A, Fares S, Wild O, Ashworth K. Current and future impacts of drought and ozone stress on Northern Hemisphere forests. *Glob Change Biol*. 2020;26:6218–6234. https://doi.org/10.1111/gcb.15339